

AEDC-TR-68-138

**ARCHIVE COPY
DO NOT LOAN**

Copy 1



**NITROGEN TETROXIDE CORROSION STUDIES
OF CRYOPANEL MATERIALS FOR SPACE CHAMBER
PROPULSION TESTING**

P. G. Waldrep and D. M. Trayer

ARO, Inc.

October 1968

This document has been approved for public release
and sale; its distribution is unlimited.

**AEROSPACE ENVIRONMENTAL FACILITY
ARNOLD ENGINEERING DEVELOPMENT CENTER
AIR FORCE SYSTEMS COMMAND
ARNOLD AIR FORCE STATION, TENNESSEE**

PROPERTY OF U. S. AIR FORCE
AEDC LIBRARY
F40600-89-C-0001

AEDC TECHNICAL LIBRARY



5 0720 0033 7604

NOTICES

When U. S. Government drawings specifications, or other data are used for any purpose other than a definitely related Government procurement operation, the Government thereby incurs no responsibility nor any obligation whatsoever, and the fact that the Government may have formulated, furnished, or in any way supplied the said drawings, specifications, or other data, is not to be regarded by implication or otherwise, or in any manner licensing the holder or any other person or corporation, or conveying any rights or permission to manufacture, use, or sell any patented invention that may in any way be related thereto.

Qualified users may obtain copies of this report from the Defense Documentation Center.

References to named commercial products in this report are not to be considered in any sense as an endorsement of the product by the United States Air Force or the Government.

NITROGEN TETROXIDE CORROSION STUDIES
OF CRYOPANEL MATERIALS FOR SPACE CHAMBER
PROPULSION TESTING

P. G. Waldrep and D. M. Trayer
ARO, Inc.

This document has been approved for public release
and sale; its distribution is unlimited. .

FOREWORD

The research presented herein was sponsored by the Arnold Engineering Development Center (AEDC), Air Force Systems Command (AFSC), Arnold Air Force Station, Tennessee, under Program Element 6240518F, Project 5730, Task 573004.

The results presented were obtained by ARO, Inc. (a subsidiary of Sverdrup & Parcel and Associates, Inc.), contract operator for AEDC under Contract F40600-69-C-0001. The research was conducted from May 1966 to May 1967 under ARO Project No. SW2607 and SW5705. The manuscript was submitted for publication on June 5, 1968.

The authors gratefully acknowledge the assistance of the Metallurgy Department of the Oak Ridge Gaseous Diffusion Plant, which is operated for the U. S. Atomic Energy Commission by Union Carbide Corporation, Nuclear Division, Oak Ridge, Tennessee. This laboratory performed the analyses of the test specimens. The authors also acknowledge the valuable assistance of S. G. Walker, W. H. Owens, and J. R. McCabe of the Chemical and Metallurgical Branch and of H. L. Henderson of the Central Engineering Branch of the Engineering Support Facility, ARO, Inc.

This technical report has been reviewed and is approved.

Eules L. Hively
Research Division
Directorate of Plans
and Technology

Edward R. Feicht
Colonel, USAF
Director of Plans
and Technology

ABSTRACT

The corrosive action of nitrogen dioxide gas and nitrogen tetroxide cryodeposit on several cryopanel metals was investigated. The specimen temperatures were periodically cycled between 77 and 300°K. The nitrogen dioxide gas pressure at ambient temperature was 4 torr. Three tests were made at different exposure periods. The basic metals tested were aluminum 1100, phosphorus deoxidized copper, and type 304L stainless steel. Weldments were made in some copper and stainless steel specimens, and an external bending stress was placed on selected specimens during the test. The degree of corrosion detected was minor and would not likely result in any structural failure of cryopanel components under similar conditions. However, some loss of the optical properties of these materials may be expected.

CONTENTS

	<u>Page</u>
ABSTRACT	iii
I. INTRODUCTION	1
II. TYPES OF CORROSION INVESTIGATED	3
III. TEST EQUIPMENT	4
IV. TEST SPECIMENS	6
V. OPERATIONAL PROCEDURES AND ANALYTICAL METHODS.	12
VI. RESULTS AND DISCUSSION	14
VII. SUMMARY AND CONCLUSIONS	18
REFERENCES.	19

TABLES

I. Stainless Steel 304L Shim Specimens.	9
II. Copper Shim Specimens	9
III. Composite Shim Specimens (304L/Cu)	10
IV. Aluminum Shim Specimens	11

APPENDIX

Illustrations

Figure

1. 1.5- by 1-ft Research Vacuum Chamber and Some Associated Equipment	23
2. N ₂ O ₄ Corrosion Test Chamber Schematic :	24
3. Corrosion Specimen Holder.	25
4. Schematic View of Specimen Stressed with Metal Strip, Mounted to Specimen Holder	26
5. Stressed Specimen Mounted on Holder	27
6. Schematic View of Specimen Stressed with Teflon Wedge, Mounted to Holder	28
7. Stressed Specimen Mounted to Specimen Holder, After Exposure.	29

<u>Figure</u>	<u>Page</u>
8. Control Specimen, Stainless Steel 304L, 500X	30
9. Control Specimen, Stainless Steel 304L at 308 ELC Weld, 500X	30
10. Stainless Steel 304L, Exposed 58 hr to Cryodeposit, 441 hr to Gas, 9 cycles, 500X	31
11. Stainless Steel 304L, Stressed, Welded with 308 ELC, Exposed 58 hr to Cryodeposit, 441 hr to Gas, 9 cycles	31
12. Stainless Steel 304L, Stressed, at 308 ELC Weld, Exposed 58 hr to Cryodeposit, 441 hr to Gas, 9 cycles, 500X	32
13. Stainless Steel 304L, Stressed, at Fusion Weld, Exposed 720 hr to Cryodeposit, 2816 hr to Gas, 20 cycles, 500X	32
14. Stainless Steel 304L, Stressed, at Fusion Weld, Exposed 720 hr to Cryodeposit, 2816 hr to Gas, 20 cycles	33
15. Stainless Steel 304L, Stressed, at 308 Rod Weld, Exposed 720 hr to Cryodeposit, 2816 hr to Gas, 20 cycles, 500X	33
16. Stainless Steel 304L, Stressed, at 347 Rod Weld, Exposed 720 hr to Cryodeposit, 2816 hr to Gas, 20 cycles, 500X	34
17. Stainless Steel 304L, at Resistance Spot Weld, Exposed 720 hr to Cryodeposit, 2816 hr to Gas, 20 cycles, 500X	34
18. Stainless Steel 304L, Welded with 304L Rod, Epoxy Coated, Exposed 58 hr to Cryodeposit, 441 hr to Gas, 9 cycles, 500X	35
19. Stainless Steel 304L, at 308 ELC Weld, Epoxy Coated, Exposed 58 hr to Cryodeposit, 441 hr to Gas, 9 cycles, 500X	35
20. Stainless Steel 304L, Fusion Welded, Exposed 420 hr to Cryodeposit, 1190 hr to Gas, 8 cycles, 3X	36
21. Brazed Copper, Contacted Copper Fin, Exposed 58 hr to Cryodeposit, 441 hr to Gas, 9 cycles, 2X.	36

<u>Figure</u>	<u>Page</u>
22. Control Specimen, Unbrazed Copper, 500X	37
23. Unbrazed Copper, Contacted Copper Fin, Exposed 58 hr to Cryodeposit, 441 hr to Gas, 9 cycles, 500X	37
24. Brazed Copper, Contacted Copper Fin, Exposed 420 hr to Cryodeposit, 1190 hr to Gas, 8 cycles, 500X	38
25. Unbrazed Copper, Contacted Aluminum Fin, Exposed 720 hr to Cryodeposit, 2816 hr to Gas, 20 cycles, 500X	38
26. Brazed Copper Control, at Braze Weld, 500X.	39
27. Brazed Copper at Braze Weld, Exposed 58 hr to Cryodeposit, 441 hr to Gas, 9 cycles, 500X.	39
28. Brazed Copper at Braze Weld, Exposed 420 hr to Cryodeposit, 1190 hr to Gas, 8 cycles, 500X	40
29. Brazed Copper at Braze Weld, Exposed 720 hr to Cryodeposit, 2816 hr to Gas, 20 cycles, 500X.	40
30. Composite Specimen, Copper Tip, Exposed 58 hr to Cryodeposit, 441 hr to Gas, 9 cycles, 2X	41
31. Composite Specimen, Stainless Steel Tip, Exposed 58 hr to Cryodeposit, 441 hr to Gas, 9 cycles, 2X.	41
32. Composite Specimen, Stainless Steel Side, Exposed 58 hr to Cryodeposit, 441 hr to Gas, 9 cycles, Stressed, 500X	42
33. Composite Specimen, at Weld on Stainless Steel Side, Exposed 58 hr to Cryodeposit, 441 hr to Gas, 9 cycles, Stressed, 500X	42
34. Composite Specimen, at Weld on Copper Side, Exposed 58 hr to Cryodeposit, 441 hr to Gas, 9 cycles, Stressed, 500X	43
35. Composite Specimen, Copper Side, Exposed 58 hr to Cryodeposit, 441 hr to Gas, 9 cycles, Stressed, 500X	43
36. Aluminum, Contacted Aluminum Fin, Exposed 720 hr to Cryodeposit, 2816 hr to Gas, 20 cycles, 3X	44

<u>Figure</u>	<u>Page</u>
37. Aluminum, Contacted Copper Fin, Exposed 58 hr to Cryodeposit, 441 hr to Gas, 9 cycles, 2X	44
38. Control Specimen, Aluminum, 500X	45
39. Aluminum, Contacted Copper Fin, Exposed 58 hr to Cryodeposit, 441 hr to Gas, 9 cycles, 500X	45
40. Aluminum, Contacted Aluminum Fin, Exposed 720 hr to Cryodeposit, 2816 hr to Gas, 20 cycles, 3X	46
41. Aluminum, Contacted Aluminum Fin, Exposed 720 hr to Cryodeposit, 2816 hr to Gas, 20 cycles, 500X	46
42. Aluminum, Contacted Copper Fin, Exposed 720 hr to Cryodeposit, 2816 hr to Gas, 20 cycles, 500X	47
43. Control Specimen, Stainless Steel Cryopanel Section, 500X	47
44. Stainless Steel Cryopanel Specimen, Exposed 58 hr to Cryodeposit, 441 hr to Gas, 9 cycles, 500X	48
45. Copper Cryopanel, Uncoated Side, Exposed 298 hr to Cryodeposit, 1629 hr to Gas, 12 cycles, 3X	48
46. Control Copper Cryopanel Specimen, Uncoated Side, 500X	49
47. Copper Cryopanel, Uncoated Side, Exposed 298 hr to Cryodeposit, 1629 hr to Gas, 12 cycles, 500X	49
48. Control Copper Cryopanel, Epoxy-Coated Side, 500X	50
49. Copper Cryopanel, Coated Side, Exposed 298 hr to Cryodeposit, 1629 hr to Gas, 12 cycles, 500X	50

SECTION I INTRODUCTION

During rocket engine testing in space simulation chambers, the internal cryogenic system will be subjected to intimate contact with raw propellants and reaction products. Such contact can lead to corrosion of the chamber components, especially with hypergolic propellants which by their nature are very reactive. The nature and extent of such corrosion damage are not assuredly predictable from published data and practical information.

Some characteristics of materials corrosion and compatibility with rocket propellants have been reported (Ref. 1). The conditions under which such corrosion data are obtained seldom approximate that of a cryogenic system operating in a space chamber during rocket firings. An extrapolation of this type of data to space chamber conditions cannot reliably be done. Vacuum conditions and wide-range temperature fluctuations will subject the cryogenic surfaces to stresses and situations under which corrosion studies have seldom been performed.

The effects of vacuum on passivity of metals, on corrosion films, on desorption of volatile corrosion products, and on adhesion properties of protective coatings (especially with absorbed corrodent present) have not been established sufficiently to predict their significance in corrosion. There are indications that a passive film may become thinner in a vacuum (Ref. 2); this might facilitate attack by a corrodent on the metal substrate. Loss of adhesion properties of corrosion films in a vacuum would likewise subject the underlying metal to continued corrosion. An absorbed corrodent could weaken the bond between a metal surface and a protective organic coating; this might result in loosening of the coating and exposure of the metal to corrosive attack. Knowledge of the effects of vacuum on properties known to be important in corrosion processes (Refs. 3, 4, and 5) is necessary in understanding the nature of corrosion occurring in space chambers used for propulsion tests.

Temperature fluctuations may be of prime importance because of the probability of a shift in direction or severity of the corrosion reaction and temperature-associated physical properties. Temperature variation definitely affects surface reactivity and reaction rates. Differences in thermal expansion between the metal and corrosion films (or passivation films) could lead to spalling, cracking, or blistering of the films to bring about further corrosion of the metal.

The purpose of this work was to perform preliminary tests of cryo-panel materials in a relatively strong single-propellant environment, both at ambient and liquid-nitrogen (LN₂) temperatures and with the application of vacuum to the test surfaces. Some factors, such as the influence of solar and ionizing radiation and exposure to propellant mixtures and reaction products, were purposely omitted from this work. These were intended as subjects for further investigation in case the findings of this study indicated a need for a more detailed examination.

Nitrogen tetroxide (N₂O₄) was used as the corrodent since it is an apt candidate for the oxidizer in space simulation chamber rocket propulsion tests. The temperature was cycled between LN₂ (77°K) and ambient (near 300°K). Chamber pressure was varied between 10⁻⁶ torr during pumping to approximately 4 torr of nitrogen dioxide (NO₂)* pressure at room temperature. The oxidizer gas pressure was at the upper limit of anticipated cell pressure of corrodent in an actual propulsion test chamber. It corresponded roughly to the pressure which would result if fuel flow to the engine failed and unreacted oxidizer dumped into the chamber for a maximum time before shutdown.

The types of metals, alloys, weldments, and coatings used were as follows:

1. Stainless steel 304L, both unwelded and welded with various rods, stressed and unstressed, uncoated and coated with a black epoxy paint,
2. 1100 aluminum,
3. Phosphorus deoxidized copper, plain and brazed with phosphor bronze, stressed and unstressed,
4. Copper welded to stainless steel 304L, stressed and unstressed,
5. Stainless steel cryopanel section, and
6. Copper cryopanel sections coated on one side with a black epoxy paint.

*At room temperature and 4 torr pressure, approximately 87 percent of the gas is present as NO₂ in equilibrium with N₂O₄ gas and other minor oxides of N₂.

SECTION II

TYPES OF CORROSION INVESTIGATED

Metallic corrosion may be defined as the destruction of a metal by chemical change, electrochemical change, or physical dissolution. Corrosion occurs in several forms and at varying rates, depending on a number of factors. These factors may include the chemical and physical nature of the metal, the presence of structural stresses, the reactivity and physical state of the corrodent, the concentration of the corrodent, the presence of other contaminants, the exposure time, and the temperature. These might act in any combination to bring about various types of corrosion.

Although this study did not attempt to cover all types of corrosion, the major types were investigated as an extension of previous work (Refs. 6 and 7). These were: general or uniform corrosion, pitting, intergranular corrosion, and stress corrosion cracking.

2.1 GENERAL OR UNIFORM CORROSION

This type of corrosion exists whenever a metal or alloy is converted fairly uniformly over the entire exposed area (Ref. 3) into corrosion products. The rate of general corrosion is usually expressed as a penetration rate in terms of thickness or weight of metal reacted per unit area per unit time. Unless this type of corrosion is exceptionally rapid, it is not usually as serious in a structural sense as microstructural damage from pitting, intergranular corrosion, and stress corrosion cracking. It may, nevertheless, result in considerable changes in the optical properties of the surface, e. g., emissivity and absorptivity.

2.2 PITTING

Pitting is a localized type of corrosion, the rate being greater in some areas as compared with other areas (Ref. 4). It is an electrochemical process in which a breakdown of metal passivity occurs at favored nuclei on the surface and proceeds beneath the surface at these sites. Pitting is a serious form of corrosion because the metal may be penetrated relatively rapidly. Practical methods are available for reducing pitting in the control of the environment and by pretreatment of the metal surface (Refs. 4 and 8). Assessment of pit depth is most commonly done by direct optical measurement of individual pits followed by statistical interpretations (Refs. 3 and 9). In some instances evaluation is based on the depth of the deepest pit.

2.3 INTERGRANULAR CORROSION

Intergranular corrosion is a serious form of localized microstructural damage in which preferential reaction occurs at the grain boundaries within a metal structure (Ref. 8). Catastrophic reduction in mechanical strength may result from intergranular corrosion (Ref. 4). This type of corrosion usually arises from the presence of impurities at the grain boundaries or from the impoverishment of critical elements (such as chromium in stainless steel alloys) within the grain boundaries.

Welding operations sometimes induce susceptibility to intergranular corrosion, particularly in areas adjacent to the weld. Intergranular corrosion is most commonly evaluated by microscopic examination of metallographic cross sections of the specimens.

2.4 STRESS CORROSION CRACKING

Stress corrosion cracking occurs as a result of the simultaneous actions of stress and corrosion (Ref. 3). The cracks may extend along grain boundaries (intergranular) or across the grain (transgranular). The term "stress corrosion cracking" is applied correctly only when the damage exceeds that resulting from stress and corrosion acting independently. The stresses involved may be either residual or applied. Most structural metals are subject to stress corrosion cracking to some extent (Ref. 4). Fortunately, however, it becomes serious only for a limited number of metals such as aluminum alloys, stainless steels, and magnesium alloys (Ref. 3). Stress corrosion cracking is more dangerous than intergranular corrosion because of more rapid propagation of fissures. In addition, because the amount of material affected is very small, stress corrosion cracking may occur with very little visible change in the surface. It becomes apparent when metallographic cross sections are examined under optical magnification.

SECTION III TEST EQUIPMENT

3.1 CHAMBER

The 1.5- by 1-ft Research Vacuum Chamber was used for these tests. The chamber (Figs. 1 and 2, Appendix) is a stainless steel cylinder 1 ft high by 18 in. in diameter. It has a free operational volume of 57.2 liters. Two ports are provided, one in the top for

sample insertion and the other on the side for viewing. Buna-N O-rings are used for vacuum sealing the ports, lid, and bottom of the chamber.

3.2 PUMPING SYSTEM

The chamber is equipped with a mechanical pump, an ion-getter pump, and three LN₂-cooled cryogenic pumps, one of which is the specimen holder itself. The mechanical pump is trapped with an LN₂ cold trap to prevent backstreaming of oil vapor into the test chamber. The ion-getter pump has a pumping speed of about 300 liters/sec in the 10⁻⁶ torr region. The chamber could be pumped to 10⁻⁶ torr with this pump when all systems were at ambient temperature.

The three LN₂ cryopumps were used sequentially to transfer a N₂O₄ cryodeposit to the test specimens. One cryopump was a small stainless steel cylinder 1 in. in diameter and 4 in. high. It was used for the initial condensation of the corrodent in the first step of the transfer process. The second cryopump was a stainless steel cylindrical shroud surrounding the specimen holder but having no thermal contact with it. When N₂O₄ was pumped onto this shroud from the small cryopump, a reasonably uniform deposit covered the cylinder inside and out, providing a relatively uniform access for the corrodent to all specimens. Finally, the specimen holder, the third cryopump, was LN₂ cooled and the corrodent transferred to the specimens by warming the shroud.

Chamber pressures in the vacuum ranges were measured with a thermocouple gage and an ion gage. To measure the pressure of the corrodent gas, a variable reluctance pressure transducer was used. This transducer was operated in the range from 0 to 5 torr with a chart recorder readout. The reference side of the transducer was maintained at mechanical pump vacuum levels during readings. It was adjusted to the null point by pumping both reference and detection sides to the mechanical pump vacuum.

Corrodent gas was pumped from the chamber with the mechanical pump through an auxiliary LN₂-cooled cold trap.

3.3 SPECIMEN HOLDER

The holder (Fig. 3) consisted of a stainless steel cylinder 1.25 in. in diameter and 10 in. long with four metal fins welded along its length and separated by 90 deg. The metal fins served as mounts for test

specimens, the attachments being made with metal screws and bolts. One end of the specimens was sandwiched between the fin and another metal strip cut and drilled to match the fin. The fins, strips, screws, and bolts were made of stainless steel, aluminum, or copper, which permitted specimens to be in contact either with similar or dissimilar metals during exposure.

Liquid nitrogen circulated through the central cylinder of the holder during cooling cycles. Sheathed thermocouples were attached to the surface of three of the fins near the weld. These monitored the fin temperature throughout the imposed range of temperatures.

In one test a section of hollow, stainless steel cryopanel test specimen was attached to the central cylinder between two fins so that LN₂ could flow directly through it. A thermocouple was attached to the upper portion of its surface.

The holder was inserted through the top of the chamber and vacuum sealed with Buna-N O-rings. When inserted, the specimen holder was surrounded on all sides by the cylindrical LN₂-cooled shroud which was open at both bottom and top.

3.4 GAS ADDITION SYSTEM

Nitrogen tetroxide* was valved into the chamber from a stainless steel container. Stainless steel needle valves and 0.5-in. stainless steel lines were used for the transfer. Chamber pressure during gas addition was monitored by the pressure transducer.

SECTION IV TEST SPECIMENS

With the exception of actual cryopanel sections, all specimens were cut from 0.020-in. -thick shimstock. Specimens were 1 in. wide by 2 in. long. One half the length was covered during testing by the fins and strips of the specimen holder. This left an area of 2 in.² (neglecting thickness) available for exposure to the corrodent. It was necessary to

*Nitrogen tetroxide used in these tests was propellant grade oxidizer meeting the specifications of MIL-P-26539A.

bend the specimens at right angles to the holder fins to fit them into the chamber. These bends made available regions of probable residual stress in the specimens.

Some of the stainless steel specimens were rod welded. Others were fusion welded, and some had spots made with a resistance welder. Copper was tested both plain and brazed with phosphor bronze rod. Several composite specimens of stainless steel joined to copper were tested. No weldments were made on the aluminum.

Bending stress was imposed on selected specimens of the welded stainless steel, the brazed copper, and the stainless steel-copper composites. The stressing techniques are described in Section 4.2.

Some of the stainless steel specimens were spray coated on the exposed surfaces with a black epoxy paint. This coating is often used to increase the absorptivity of cryopanel surfaces.

4.1 WELDING METHODS

The weld beads were made after the specimens were cut in a direction parallel to the sample holder fin. Before welding, the two pieces were matched and clamped in a special jig. Argon (Ar) gas was fed through the jig on the underside of the weld joint to minimize oxidation at that point. All welds, except the resistance welds, were made with a DC welder using Ar shielding gas. Welding wire was hand fed during joining.

The stainless steel welds were made using approximately 0.030-in. wires. Three welding materials: 308 ELC, 308, and 347 were used in preparing different specimens. Three stainless steel specimens were prepared by fusion welding. Two specimens were tested after applying four spots with a resistance welder using a copper electrode at 100 watts/sec. These were made directly on the surface of uncut specimens so that no resistance welded joints were tested. Composite specimens of 304L stainless joined to copper were welded with nickel wire 0.030 in. in diameter. Copper specimens were joined with 0.035-in. phosphor bronze C wire (95-percent bronze, 5-percent tin).

4.2 STRESSING TECHNIQUES

As mentioned earlier, all specimens were bent at right angles to the holder fin. This deformation beyond the yield point probably resulted

in residual stresses within the specimens near the bends. Welding probably contributed further to introducing stress. Additional bending stress was imposed on selected specimens by two methods.

One technique is shown schematically in Fig. 4. A strip of 304L stainless steel 0.020 in. thick and 0.060 in. wide was inserted between two specimens facing flat against each other. After insertion of the strip, the tips of the specimens were drawn together with stainless steel bolts. A variable bending stress was exerted throughout the exposed portions of the specimens without yielding. A test specimen stressed by this method is shown in Fig. 5.

The second method of applying bending stress is shown in Figs. 6 and 7. Two specimens were bolted into the holder at the same point but separated from one another by a metal strip 0.060 in. thick. This left the surfaces parallel on both specimens. The specimens were then further separated slightly to just beyond the yield point. Stress was then applied by inserting a Teflon[®] wedge between the tips just enough to cause deflection but not enough to permanently deform the metal. The wedge was held in place by wiring each end to the sample holder.

4.3 STAINLESS STEEL SHIM SPECIMENS

A total of 37 stainless steel 304L shim specimens were tested. Thirty of these were welded specimens. A black epoxy coating was applied to six of the specimens, two of which were welded. Bending stress was imposed on 14 of the specimens, all welded. The specimens were cleaned by wire brushing all welds and oxidized areas, followed by degreasing and ultrasonic cleaning in aqueous detergent and Freon MF[®]. A list of all stainless steel specimens and their exposure conditions is given in Table I.

4.4 COPPER SHIM SPECIMENS

A total of 16 copper specimens, seven of them brazed, were tested. Three of the specimens were mounted to an aluminum holder fin. The remainder were attached to copper fins. Two brazed copper specimens were tested under imposed bending stress. The copper specimens in two tests were cleaned before testing with a commercial metal polish, followed by thorough removal of remaining film and loose oxide with multiple methanol and acetone washes. The specimens were then ultrasonically cleaned in Freon MF. In one test the specimens were cleaned by immersion in an aqueous solution of 15-percent acetic acid and

0.2-percent Rodamine[®] inhibitor at 80°C. After distilled water and acetone rinsing, the specimens were finally cleaned ultrasonically in Freon MF. Except for minor surface roughening of the acid-cleaned specimens, no significant differences were noted between specimens cleaned by each method. Table II shows the copper types and exposure conditions.

TABLE I
STAINLESS STEEL 304L SHIM SPECIMENS

Specimen Description	Number of Specimens Exposed		
	Exposed 420 hr; N ₂ O ₄ Cryodeposit, 1190 hr; NO ₂ Gas at 4 torr, Eight Temperature Cycles	Exposed 720 hr; N ₂ O ₄ Cryodeposit, 2816 hr; NO ₂ Gas at 4 torr, 20 Tem- perature Cycles	Exposed 58 hr; N ₂ O ₄ Cryodeposit, 441 hr, NO ₂ Gas at 4 torr, Nine Temperature Cycles
Plain	0	0	3
Coated*, No Weld	1	2	1
308 ELC Rod Welded	1	1	3
308 ELC Welded, Stressed	0	2	6
308 ELC Welded, Coated	0	0	2
Fusion Welded	1	1	0
Fusion Welded, Stressed	0	2	0
347 Rod Welded	1	1	0
347 Rod Welded, Stressed	0	2	0
308 Rod Welded	1	1	0
308 Rod Welded, Stressed	0	2	0
Resistance Welded	1	2	0

*Specimens designated "coated" were painted with a black epoxy.

TABLE II
COPPER SHIM SPECIMENS

Specimen Description	Number of Specimens Exposed		
	Exposed 420 hr; N ₂ O ₄ Cryodeposit, 1190 hr; NO ₂ Gas at 4 torr, Eight Temperature Cycles	Exposed 720 hr; N ₂ O ₄ Cryodeposit, 2816 hr; NO ₂ Gas at 4 torr, 20 Tem- perature Cycles	Exposed 58 hr; N ₂ O ₄ Cryodeposit, 441 hr; NO ₂ Gas at 4 torr, Nine Temperature Cycles
Plain, Contacting Copper Fin	1	2	3
Plain, Contacting Aluminum Fin	1	2	0
Brazed, Contacting Copper Fin	1	2	2
Brazed, Stressed Contacting Copper Fin	0	0	2

4.5 COMPOSITE SHIM SPECIMENS

Thirteen specimens were prepared by welding stainless steel 304L to phosphorus deoxidized copper with nickel wire. Nine of these had copper tips; that is, the portion contacting the holder fin was stainless steel 304L. The remainder had stainless steel tips with the copper portion bolted into the holder. Stress was applied to eight of these. Specimens were cleaned by wire brushing the stainless portion and the weld. The copper portion was cleaned by the inhibited acetic acid method described in the preceding section (Section 4.4). The final cleaning was done ultrasonically in Freon MF. Table III lists the types of specimens and conditions of exposure. Note that composite specimens were included in only one test.

TABLE III
COMPOSITE SHIM SPECIMENS (304L/Cu)

Exposure Conditions: 58 hr; N ₂ O ₄ Cryodeposit, 441 hr; NO ₂ Gas at 4 torr, Nine Temperature Cycles	
Specimen Description	Number of Specimens
Contacting Copper Fin, 304L Tip	2
Contacting Copper Fin, 304L Tip, Stressed	2
Contacting Stainless Fin, Copper Tip	3
Contacting Stainless Fin, Copper Tip, Stressed	6

4.6 ALUMINUM

Twelve aluminum specimens were tested. Six of these contacted copper holder fins during exposure, and the remainder contacted aluminum fins. No weldments were made and no stress was applied beyond the residual stresses of bending. The specimens were cleaned by immersion in methanol and acetone followed by ultrasonic cleaning in Freon MF solvent. Aluminum test specimens are tabulated in Table IV.

TABLE IV
ALUMINUM SHIM SPECIMENS

Specimen Description	Number of Specimens Exposed		
	Exposed 420 hr; N ₂ O ₄ Cryodeposit, 1190 hr; NO ₂ Gas at 4 torr, Eight Temperature Cycles	Exposed 720 hr; N ₂ O ₄ Cryodeposit, 2816 hr; NO ₂ Gas at 4 torr, 20 Temperature Cycles	Exposed 58 hr; N ₂ O ₄ Cryodeposit, 441 hr; NO ₂ Gas at 4 torr, Nine Temperature Cycles
Contacting Copper Fins	1	2	3
Contacting Aluminum Fins	1	5	0

4.7 CRYOPANEL SECTIONS

4.7.1 Commercial Stainless Steel Cryopanel Specimen

A section of commercially fabricated 304L stainless steel cryopanel was exposed in one test. A section 4 in. long by 2 in. wide was sawed from a new cryopanel. The edges were fusion welded and the welds wire brushed to remove scale. It was then welded to 3/8-in. stainless lines which were welded into the specimen holder so that LN₂ would circulate directly through the section during cooling. A sheathed thermocouple was attached to the surface. The welds were then wire brushed again and the entire specimen holder ultrasonically cleaned. This specimen was exposed to N₂O₄ cryodeposit for 58 hr and to NO₂ gas at a pressure of 4 torr for 441 hr. It was taken through nine temperature cycles.

4.7.2 Commercial Copper Cryopanel Specimens

Five 1- by 2-in. sections were cut from a commercially supplied copper cryopanel. These were coated on one side with a black epoxy paint and had a total thickness (including coating film) of 0.04 in. The uncoated sides were oxidized from handling, exposure to the atmosphere, and brazing. The specimens were cleaned only by wiping with a clean cloth. Three were attached to a copper holder fin and two to an aluminum fin. They were exposed for 298 hr to N₂O₄ cryodeposit and 1629 hr to NO₂ gas at 4 torr. They were taken through 12 temperature cycles.

SECTION V OPERATIONAL PROCEDURES AND ANALYTICAL METHODS

5.1 OPERATIONAL PROCEDURES

After placing the test specimens in the chamber, the chamber was pumped with the mechanical pump to the 10^{-4} torr range. The ion pump was then started and the pressure further reduced to the 10^{-6} torr range. The ion pump was then isolated before the addition of the corrodent gas.

Nitrogen dioxide gas from the N_2O_4 reservoir was then slowly added to the chamber to a pressure of approximately 4 torr, as indicated by the pressure transducer readout.

After a suitable exposure to the gas at ambient temperatures, the temperature cycling procedures were begun. This was done in a sequence which assured a practically uniform cryodeposit of N_2O_4 on the specimens. First, the small 4-in. cryopump was cooled with LN_2 until the chamber pressure equilibrated (under 0.1 torr), usually within 2 min. Then the shroud surrounding the specimen holder was cooled with LN_2 and the chamber pumped with the ion pump to the 10^{-6} torr range to minimize noncondensable gases. The small cryopump was then warmed, thereby transferring the cryodeposit to the shroud walls. The specimen temperature at this point was around 216°K. The specimen holder was cooled with LN_2 until the surface temperature equilibrated, usually around 89°K. The shroud was then warmed with a GN_2 purge. This transferred the cryodeposit to the specimens and holder. After a suitable exposure time the holder was warmed by purging with GN_2 .

After several cycles the chamber gas was pumped into an LN_2 trap for disposal. The chamber was recharged with fresh NO_2 periodically.

Upon termination of a test, the chamber gas was pumped out and the chamber pressurized with bone-dry N_2 to atmospheric pressure. The holder was removed from the chamber. The specimens were carefully removed from the holder with plastic-coated tongs and placed in vacuum desiccators for transfer to the analytical laboratory.

5.2 ANALYTICAL METHODS

All analyses performed on the test specimens were performed by the Technical Division of the Oak Ridge Gaseous Diffusion Plant which

is operated for the U. S. Atomic Energy Commission by the Nuclear Division of Union Carbide Corporation in Oak Ridge, Tennessee. The methods employed by this laboratory to evaluate the extent of corrosion included metallographic examination by optical microscopy, X-ray diffraction, nitrogen analysis, electron probe microanalysis, and infrared spectrophotometry.

5.2.1 Metallographic Specimen Preparation and Examination

The surfaces of all specimens were examined as a preliminary step at low magnification (10X to 40X) under a stereomicroscope. If this examination revealed questionable areas or areas of certain corrosive action, the specimen was selected for more detailed metallographic examination. Selected specimens were photographed at 2X to 3X magnification.

Metal sections of interest were cut into 0.25-in.-wide strips and mounted in a room-temperature curing epoxy resin. After mounting, the samples were wet ground on abrasive papers to remove the effects of cutting and to prepare them for polishing.

Rough polishing was done on rotating laps with diamond abrasives. Following this, specialized methods of polishing and etching were used, as called for by the particular type of metal under examination.

Stainless steel specimens were polished on a vibratory polisher with 0.3- μ alumina suspended in ethylene glycol. They were finished by hand on polishing cloth with 0.05- μ alumina abrasive. After examination of the cross sections at high magnification (up to 1000X), they were electrolytically etched in 10-percent oxalic acid at 6 volts (specimen anodic). They were then photographed at high magnification with a research metallograph.

Copper specimens were final polished on the vibratory polisher with 0.3- μ alumina in ethylene glycol followed by hand polishing on cloth with 0.05- μ alumina in a dilute ammonia solution. These specimens were microscopically examined and then etched with ASM No. 4 etch for copper and copper alloys for photomicrography on the metallograph.

Aluminum specimens were polished with levigated alundum on polishing cloth and finished with magnesia on polishing cloth. Aluminum samples were microscopically examined and photographed without etching.

5.2.2 X-Ray Diffraction

X-ray diffraction analyses were made on surface scrapings of selected specimens in attempts to establish the identity of the corrosion films. The scrapings were placed in a Debye-Scherrer powder camera used together with a Philips X-ray generator with diffraction tube. Nickel-filtered $\text{CuK}\alpha$ radiation was used at 45 kvp and 20 ma.

5.2.3 Nitrogen Analysis

Nitrogen was determined in the corrosion product from several specimens by a micro-Kjeldahl colorimetric method. The nitrates in the corrosion film were reduced to ammonia by digesting in an acidic hydrogen peroxide solution. The solution was then made alkaline and the ammonia separated by steam distillation. The distillate was then quantitatively analyzed for ammonia by a spectrophotometric method using Nessler's reagent for color development.

5.2.4 Electron Probe Microanalysis

This technique permits elemental analysis of corrosion films on the surface of the metal specimen itself. Selected areas of some exposed specimens were scanned for nitrogen with a Philips Electron Probe Microanalyzer. The electron beam was operated at 30 kv. The beam size was adjusted to $50\ \mu$. The electron microprobe analysis technique is discussed in Ref. 10, and a brief description is presented in Refs. 11 and 12.

5.2.5 Infrared Absorption Spectral Analysis

The exposed stainless steel specimens had a translucent film present after N_2O_4 exposure. In an effort to identify this film, 12 specimens were selected and the film extracted with acetone for infrared analysis. The acetone solution was evaporated to dryness on a glass slip and an infrared absorption pattern made using a Beckman IR 12 spectrophotometer.

SECTION VI RESULTS AND DISCUSSION

6.1 STAINLESS STEEL 304L SHIM

Metallographic examination of representative specimens showed no evidence of substantial microstructural corrosion of any type in the base

metal, at the welds, in heat-affected zones, or beneath the epoxy coating. Likewise, no effect was noted in any areas as a result of imposed or residual stresses. Especially close attention was given to bend areas and areas where abnormal surface features were noted. Figures 8 and 9 show cross-sectional photomicrographs of unexposed control specimens. For comparison, Figs. 10* through 19 show cross sections of exposed specimens of the types tested.

All of these specimens, including the unexposed control, showed a slight grain boundary notching at the surface. Since this occurred also in unexposed specimens, it is concluded that these defects were formed during manufacture and do not indicate corrosion activity.

The corrosion product visible in the cross section of the resistance welded specimen, Fig. 17, resulted from attack on copper deposited at the weld from the welding electrode.

A transparent film developed on many of the stainless steel specimens during exposure, Fig. 20. This film was easily removed by washing with acetone or water, revealing an apparently unaffected substrate. Metallographic examination of cross sections verified the integrity of the underlying metal. Doubtless, such a film might change the optical properties to an undetermined extent. Infrared analysis of acetone extracts from 12 of these specimens identified one constituent of the film as a silicone lubricant. The source of the silicone was unknown. However, it was present in such small amounts that it could have come from a very minor source. The nitrogen content as measured by the micro-Kjeldahl method was too low to make a meaningful estimation of penetration depth, if any. The X-ray diffraction analysis of the films yielded good patterns but was inconclusive since no match could be made with available standards.

6.2 COPPER SHIM SPECIMENS

A grey to green general corrosion deposit formed on all the copper specimens. This is shown in Figs. 7 and 21. The film caused a loss of metallic luster and would definitely cause a change in the optical characteristics of the surface. The film was deliquescent and appeared to undergo a chemical change (probably hydrolysis from atmospheric

*The grey zone between the metal surface and the mounting resin in Fig. 10 was caused by mixing of the mounting resin and the surface film which was particularly abundant at the site of this photograph.

moisture) when the specimens were removed from the test chamber. This final product was identified by X-ray diffraction as a tribasic copper (II) nitrate, $\text{Cu}_2(\text{OH})_3\text{NO}_3$.

This general corrosive attack caused a slight roughening of the underlying copper shim. Figures 22 through 25 show cross sections of the copper shim for a control specimen and for three test specimens exposed for increasing time periods. The surface roughening is seen to increase with exposure time but is not structurally serious even for the specimen exposed longest, Fig. 25. Here the roughening had extended to a maximum depth of only $5\ \mu$. There is no evidence of sharply localized attack, such as pitting or intergranular corrosion, on the copper shim itself. However, the brazed specimens exposed for the longer periods did show some pitting in the braze joints. These pits, or voids, were formed in regions where the tin content had been enriched by severe segregation of the phosphor bronze during nonequilibrium cooling in the welding operation. The maximum pit depth observed in the welds was $64\ \mu$. This pitting action did not extend into the copper adjacent to the welds. No other types of microstructural corrosion damage were noted.

Cross sections of welds in unexposed control specimens, Fig. 26, clearly showed the metal segregation. The tin-rich areas appear darker against a background of tin-deficient metal. The grain size enlargement near the weld was caused by welding heat. Comparison of control and test specimens strongly suggests a positive relationship between the degree of pitting and the time of exposure to the oxidizer. Figures 27 through 29 show the phosphor bronze welds in specimens exposed for increasing time periods. The severity of pitting is seen to increase with exposure time. This attack could possibly be prevented by more carefully controlled cooling during brazing or by selection of a brazing material of a more compatible composition.

The degree of corrosive attack on the copper and the braze welds appeared to be unaffected by stressing or by contact with a dissimilar metal (aluminum).

6.3 COMPOSITE SHIM SPECIMENS 304L/COPPER

The stainless steel and copper parts of the composite specimens had approximately the same behavior with the oxidizer as did separate specimens of the same metals. The stainless steel portions showed no evidence of attack of any type. The copper portions were covered with a light corrosion film similar to the film which formed on the all-copper

specimens. A lighter corrosion film covered the nickel welds. Two representative composite specimens are pictured in Figs. 30 and 31. No pitting, intergranular corrosion, or stress corrosion was seen in either the base metals or the welds. Photomicrographs of a typical composite test specimen are shown in Figs. 32 through 35.

6.4 ALUMINUM SHIM

Only three of the 11 aluminum specimens tested showed signs of significant corrosive attack. Most specimens retained their original metallic luster, Figs. 36 and 37. Some were covered by a thin, transparent film, which had no apparent effect on their brightness. The film was too sparse for definite identification.

Metallographic examination and comparison with controls revealed a slightly roughened surface caused by exposure, Figs. 38 and 39. No microstructural damage was found. No difference was noted between those specimens contacting copper fins and those contacting aluminum during exposure.

Three specimens were found to differ from those just described. Two of these had lost some of their brightness and were covered with scattered dark spots, Fig. 40, indicating some general corrosive attack. Photomicrographs, Fig. 41, showed moderate surface roughening. The dark spots apparently were caused by accumulation of corrosion product in areas of incipient pit formation. These pits were very shallow (about 2μ), but based on the corrosion deposit at each pit site, they might be expected to deepen as exposure continued. A third specimen, although retaining its bright luster, had suffered a different type of pit formation. A cross-sectional photograph showing such a pit is shown in Fig. 42. An angular, irregular pit, typical of corrosion pits, is situated within a larger, smooth pit. Judging from its smooth features, the larger pit was formed by mechanical damage before testing. The damage probably left relatively active worked metal surfaces where corrosion pit formation could initiate. Pre-exposure passivation would be indicated as a preventive measure against this type of pitting in uncoated aluminum cryopanel.

6.5 STAINLESS STEEL CRYOPANEL SECTION

Photomicrographs of the stainless steel cryopanel section before and after exposure are shown in Figs. 43 and 44. The exposed specimen was coated with a thin film similar to the film on the stainless steel shim

specimens. However, metallographic examination revealed no evidence of corrosive attack on the cryopanel as a result of exposure. The pits visible in the micrographs are surface irregularities incurred in the production of the cryopanel.

6.6 COPPER CRYOPANEL SECTIONS

Since only one side of these specimens was coated with the protective epoxy paint, a comparison could be made between unprotected and protected copper surfaces. The uncoated sides underwent some general corrosion, as evidenced by the presence of corrosion products on the surface, Fig. 45. Figures 46 and 47 show photomicrographs of a control specimen and a test specimen, respectively. The surface roughness is typical of both specimens. Judging from the strain lines observed at the surface of these irregularities, the surface roughness appears to have resulted from abrasive cleaning during manufacture of the metal. Abrasive blasting with sand or grit causes such strain lines in the copper by work hardening. No localized corrosive attack was noticed.

The black epoxy coating fully protected the underlying copper from corrosion. Photomicrographs of control and test specimen sections showing coated sides are shown in Figs. 48 and 49. Surface roughness similar to that seen on the uncoated side is apparent on both specimens. Abrasive cleaning was probably employed as a preparation for application of the coating.

While the epoxy coating protected the copper surface from corrosion, it was not completely impervious to the oxidizer. When the test specimens were cut on an abrasive wheel before metallographic mounting, the odor of NO_2 was very evident. This indicates an absorption of oxidizer in the epoxy film. If this were true, an underlying surface of sufficiently high reactivity would experience corrosion despite the coating.

SECTION VII SUMMARY AND CONCLUSIONS

From this exploratory corrosion study with N_2O_4 , the results and conclusions are summarized by the following statements. Application of these results to other conditions should not be made without further work with appropriate variables.

1. Phosphorus deoxidized copper exhibited general corrosion with some surface roughening after a period of time. Pitting to an observed maximum depth of $64\ \mu$ occurred in tin-enriched areas of welds made with phosphor bronze (95-percent bronze, 5-percent tin). The exposure caused a considerable reduction in the surface brightness of the copper.
2. Stainless steel 304L, welded and unwelded, stressed and unstressed, coated with an epoxy and uncoated, presented no detectable general or localized corrosion. A light film was formed on the exposed surfaces. This could cause changes in the optical properties of the metal.
3. Aluminum generally had good corrosion resistance, but a few findings indicated some possible problems. With one specimen, general corrosion with loss of some surface reflectivity and a moderately roughened surface together with incipient pit formation were observed.
4. The welded copper-stainless steel composites generally had the same corrosion characteristics in their component parts as the individual materials. No detectable significant corrosion was found in these specimens.
5. Evidence suggests that a black epoxy coating absorbs N_2O_4 . The absorbed gas may lengthen pumpdown time when the cryopanel is warm.
6. A basic copper (II) nitrate, $Cu_2(OH)_3NO_3$, was identified by X-ray diffraction as a corrosion product from copper. The original deliquescent salt apparently is converted into the identified compound by atmospheric moisture.
7. Based on the results of these tests, stainless steel 304L and 1100 aluminum appear to be superior to phosphorus deoxidized copper for cryopanel intended for use in an N_2O_4 environment.

REFERENCES

1. "Compatibility of Materials with Rocket Propellants and Oxidizers." Defense Metals Information Center, Battelle Memorial Institute, Columbus, Ohio, DMIC Memorandum 201, January 1965.

2. Andreeva, V. V. "Behavior and Nature of Thin Oxide Films on Some Metals in Gaseous Media and In Electrolyte Solutions." Corrosion, Vol. 20, No. 2, 1964, pp. 35t-46t.
3. Evans, V. R. The Corrosion and Oxidation of Metals: Scientific Principles and Practical Applications. Edward Arnold Limited, London, 1960.
4. Uhlig, H. H. Corrosion and Corrosion Control. John Wiley & Sons, Inc., New York, 1963.
5. Adamson, A. W. Physical Chemistry of Surfaces. Interscience Publishers, New York, 1960.
6. Waldrep, P. G. "Nitrogen Tetroxide-Stainless Steel Cryopanel Corrosion and Coating Degradation in Space Chamber Propulsion Testing." AEDC-TR-66-226 (AD650690), April 1967.
7. Waldrep, P. G. "Cryopanel Corrosion and Coating Degradation in Space Chamber Propulsion Testing." AIAA/IES/ASTM Space Simulation Conference, Houston, Texas, September 7-9, 1966, p. 127.
8. Uhlig, H. H. The Corrosion Handbook. John Wiley & Sons, Inc., New York, 1948.
9. Champion, F. A. Corrosion Testing Procedures. John Wiley & Sons, Inc., New York, 1965.
10. Birks, L. S. Electron Probe Microanalysis. Interscience Publishers, New York, 1963.
11. Chalmers, B. and Quarrell, A. O. (Ed.) The Physical Examination of Metals. (Second Edition). Edward Arnold Limited, London, 1960.
12. Kehl, O. L. The Principles of Metallographic Laboratory Practice. (Third Edition). McGraw-Hill Book Company, Inc., New York, 1949.

**APPENDIX
ILLUSTRATIONS**

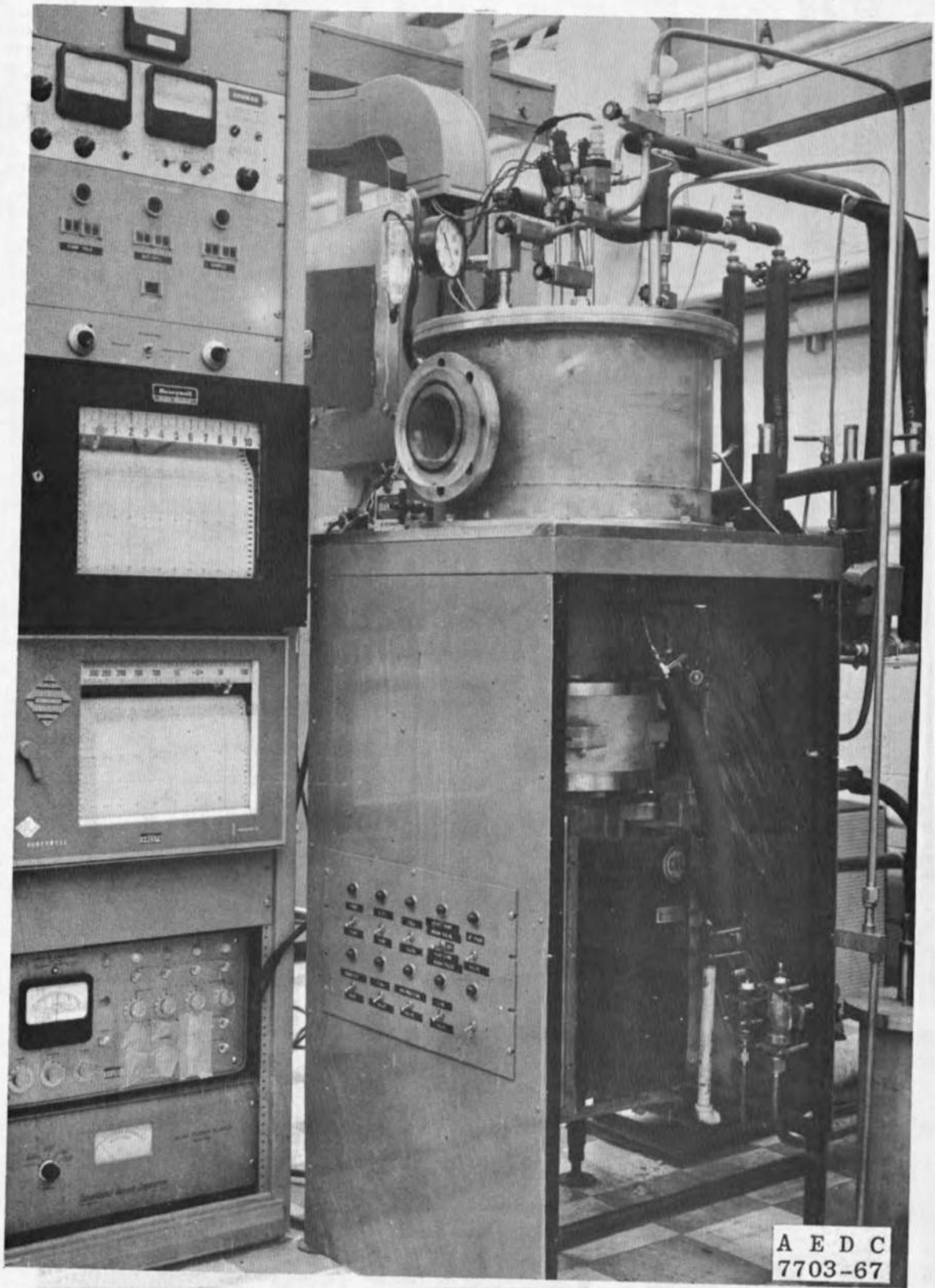


Fig. 1 1.5-by 1-ft Research Vacuum Chamber and Some Associated Equipment

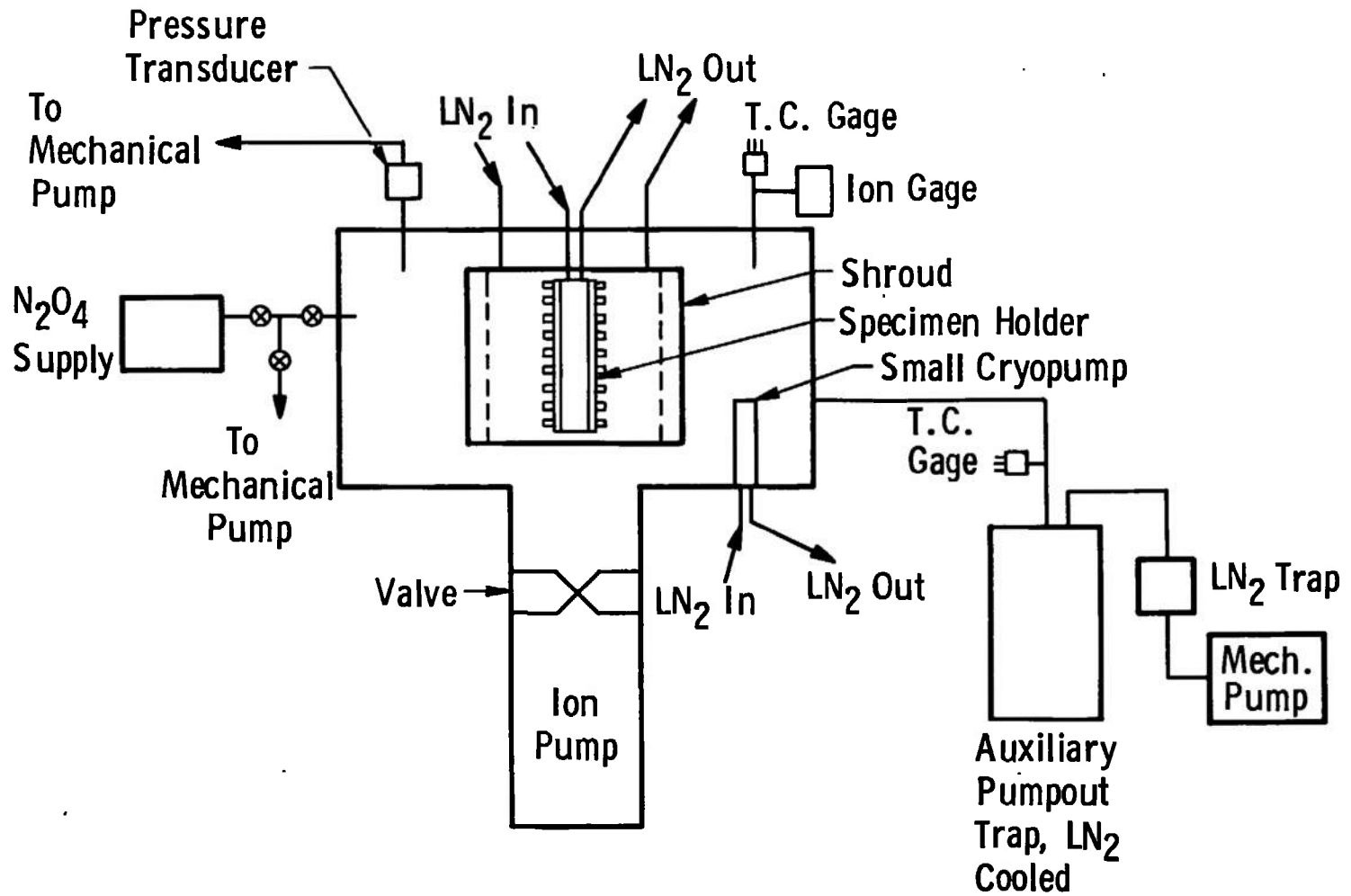


Fig. 2 N_2O_4 Corrosion Test Chamber Schematic

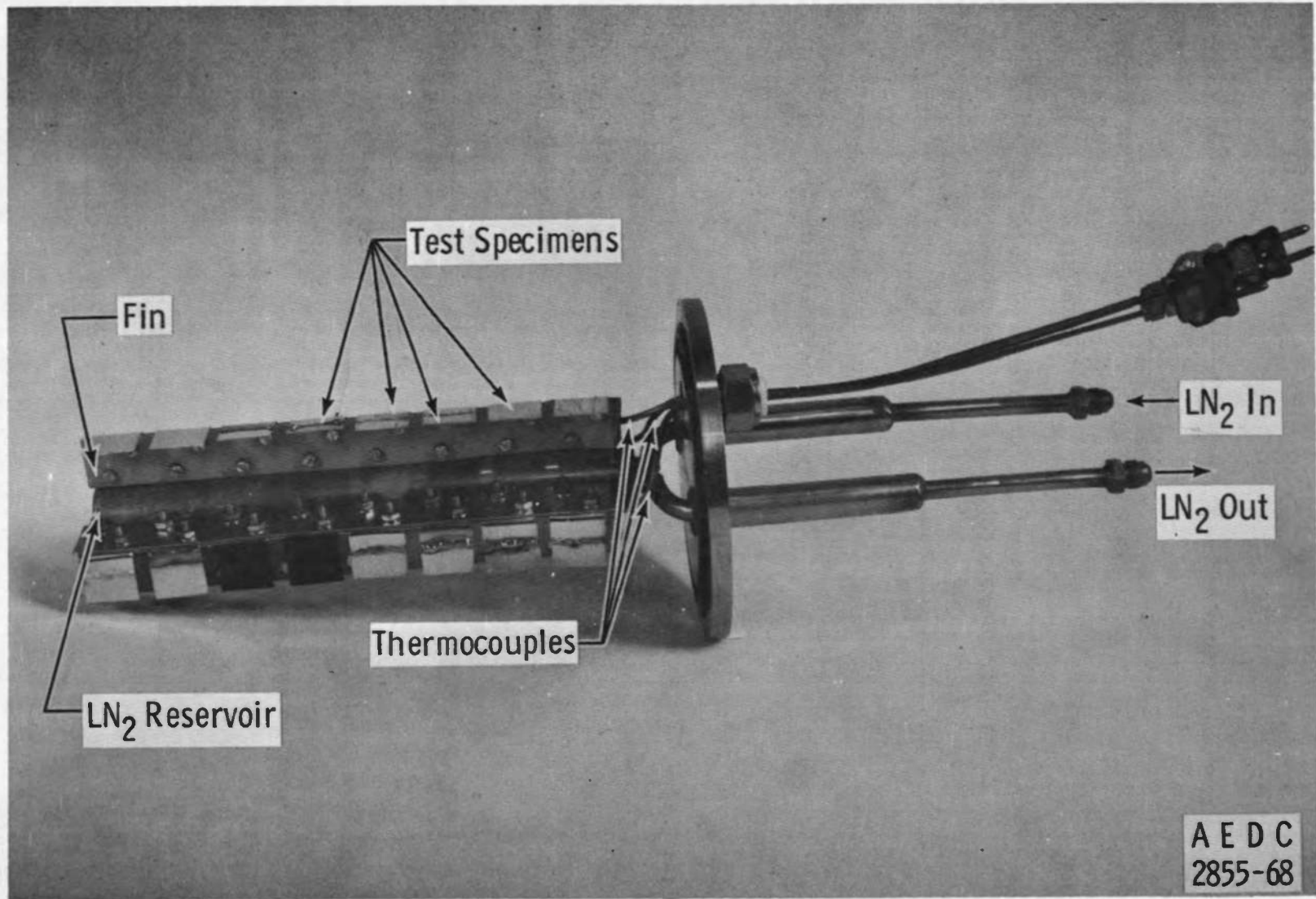


Fig. 3 Corrosion Specimen Holder

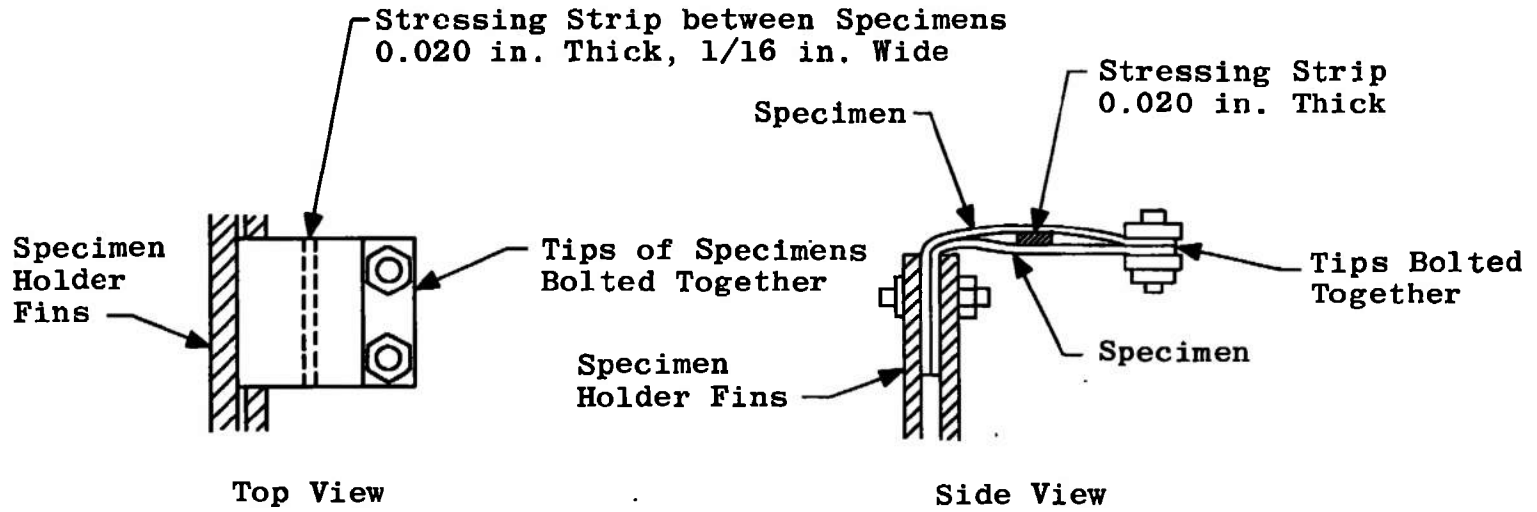


Fig. 4 Schematic View of Specimen Stressed with Metal Strip, Mounted to Specimen Holder

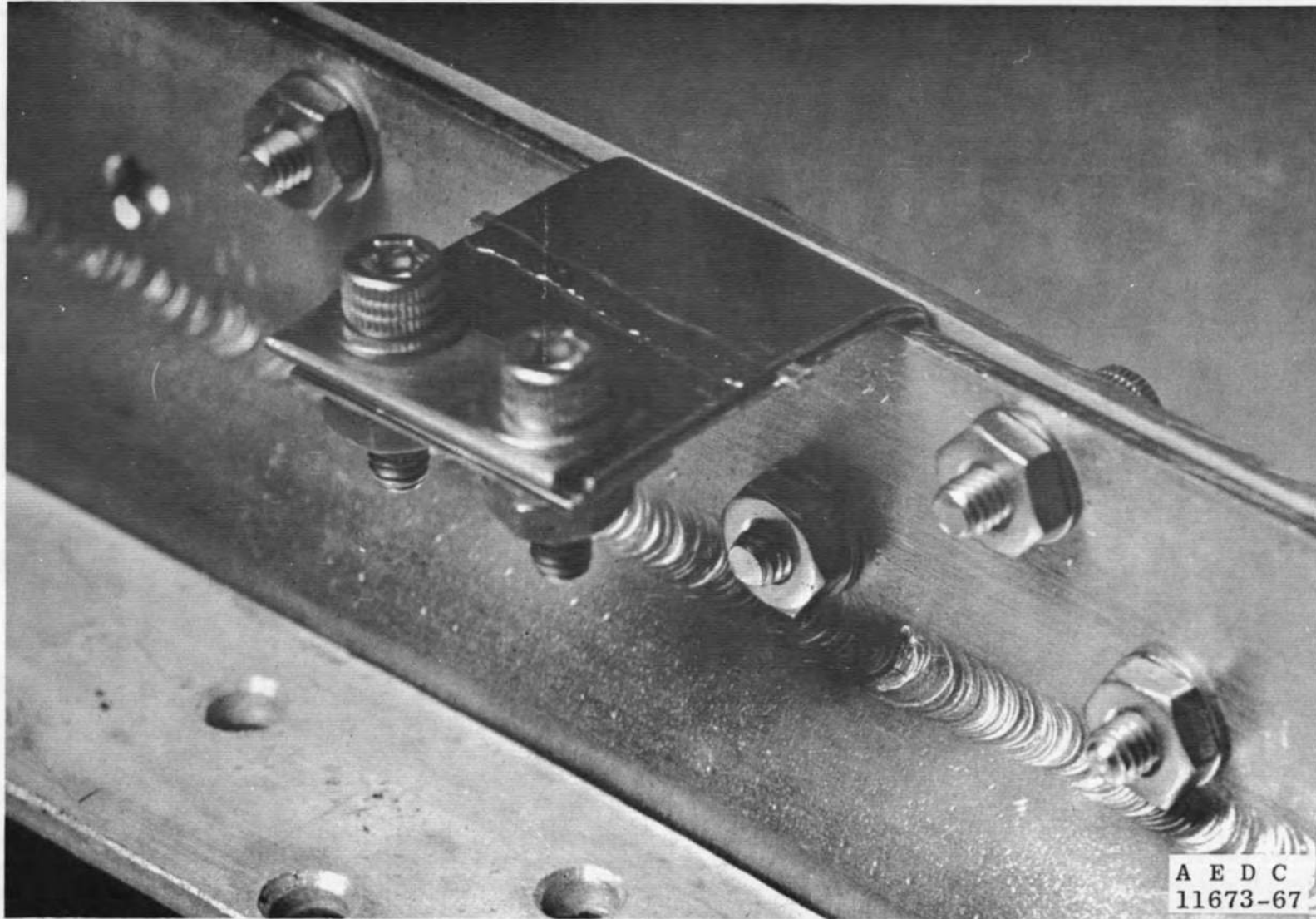


Fig. 5 Stressed Specimen Mounted on Holder

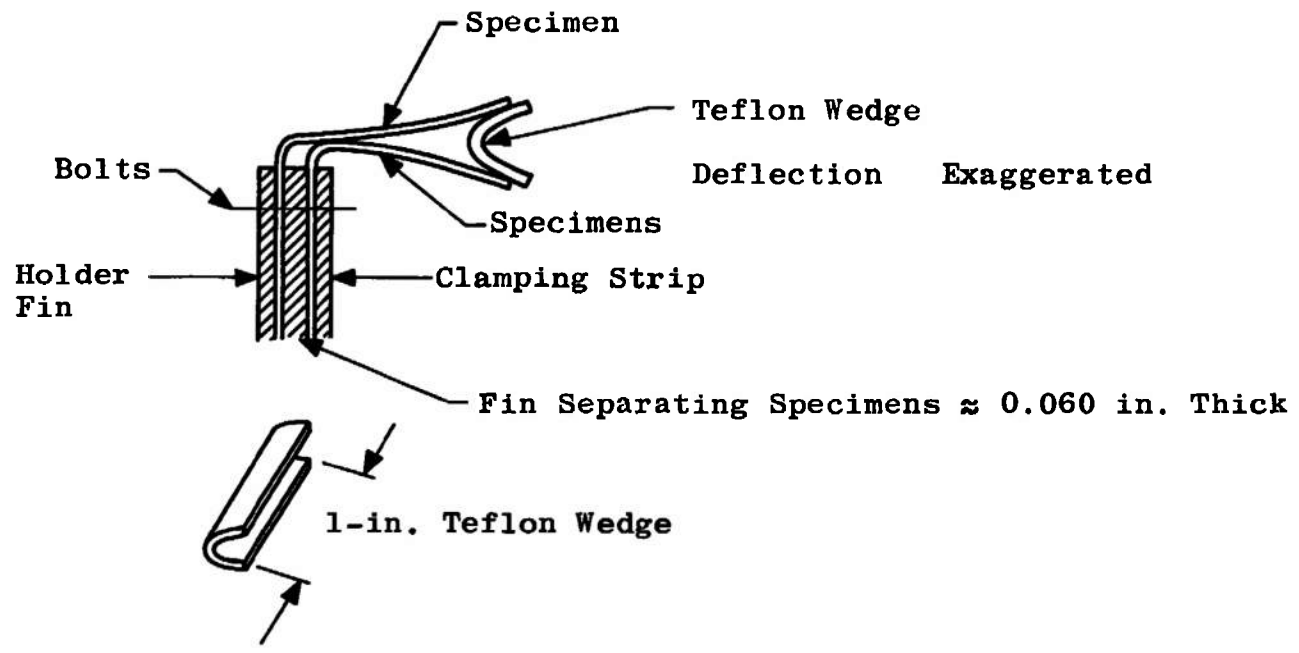


Fig. 6 Schematic View of Specimen Stressed with Teflon Wedge, Mounted to Holder

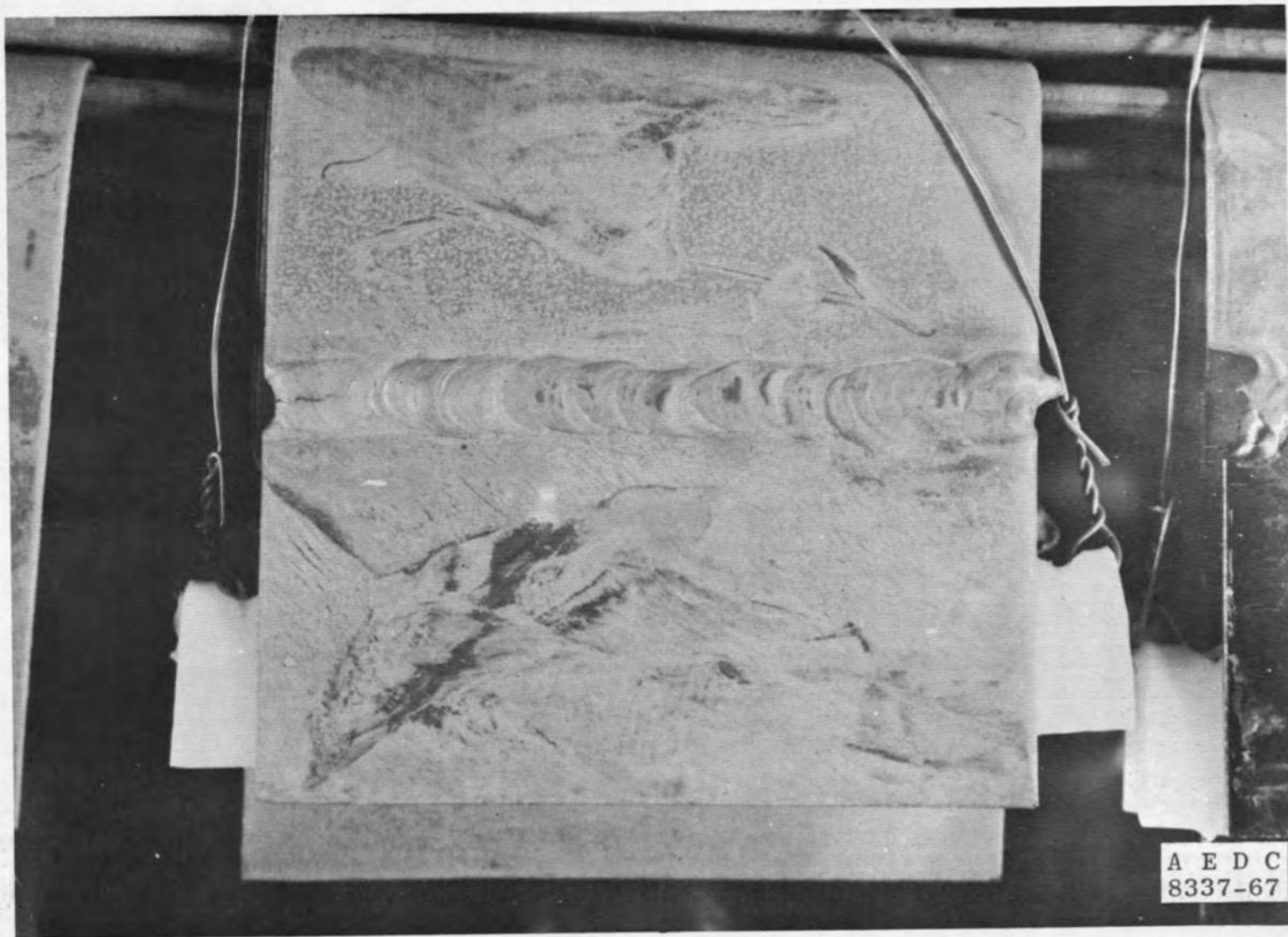


Fig. 7 Stressed Specimen Mounted to Specimen Holder, After Exposure



Fig. 8 Control Specimen, Stainless Steel 304L, 500X

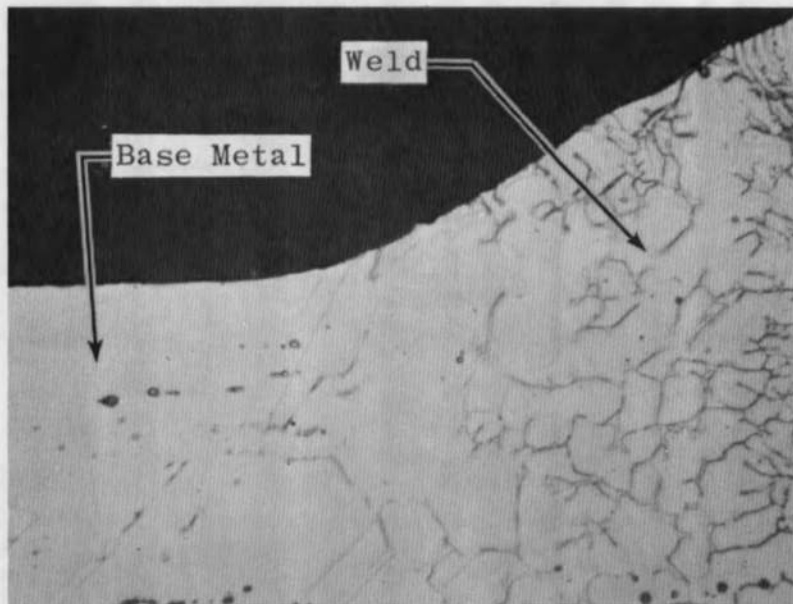


Fig. 9 Control Specimen, Stainless Steel 304L at 308 ELC Weld, 500X



Fig. 10 Stainless Steel 304L, Exposed 58 hr to Cryodeposit, 441 hr to Gas, 9 cycles, 500X



Fig. 11 Stainless Steel 304L, Stressed, Welded with 308 ELC, Exposed 58 hr to Cryodeposit, 441 hr to Gas, 9 cycles

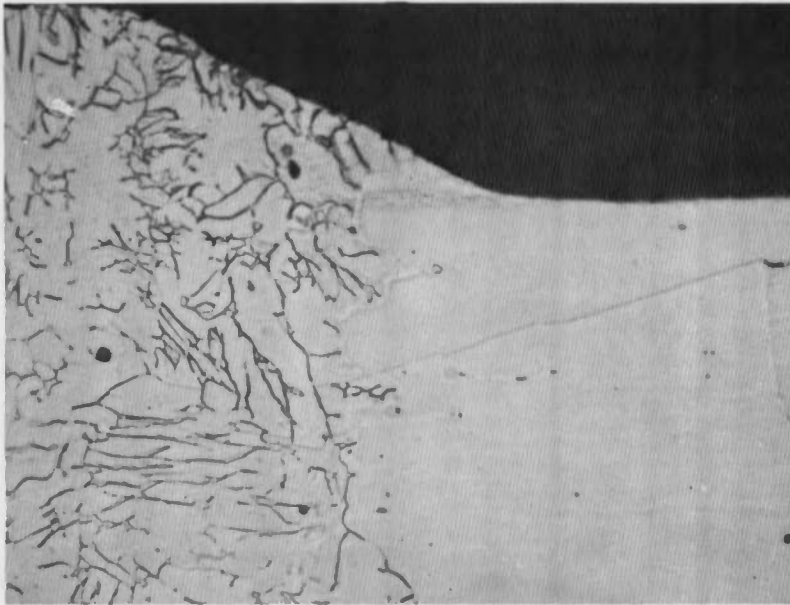


Fig. 12 Stainless Steel 304L, Stressed, at 308 ELC Weld, Exposed 58 hr to Cryodeposit, 441 hr to Gas, 9 cycles, 500X



Fig. 13 Stainless Steel 304L, Stressed, at Fusion Weld, Exposed 720 hr to Cryodeposit, 2816 hr to Gas, 20 cycles, 500X

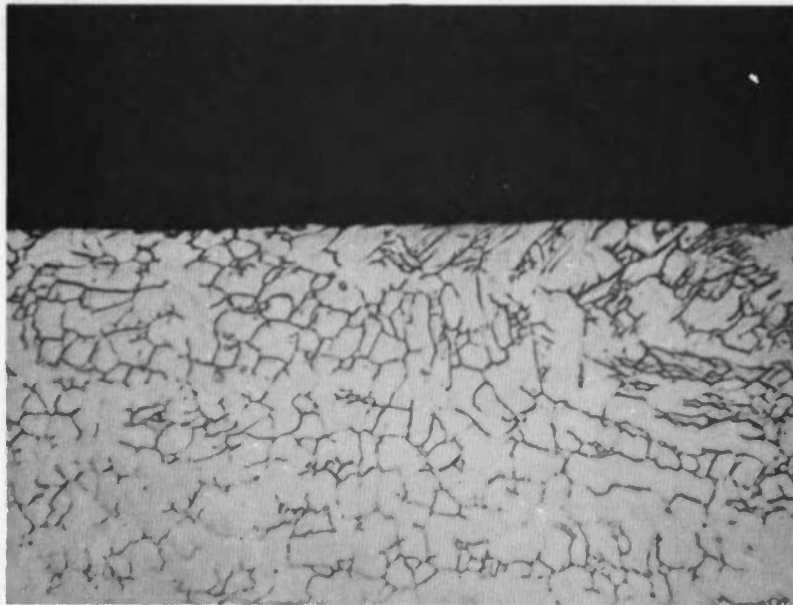


Fig. 14 Stainless Steel 304L, Stressed, at Fusion Weld, Exposed 720 hr to Cryodeposit, 2816 hr to Gas, 20 cycles

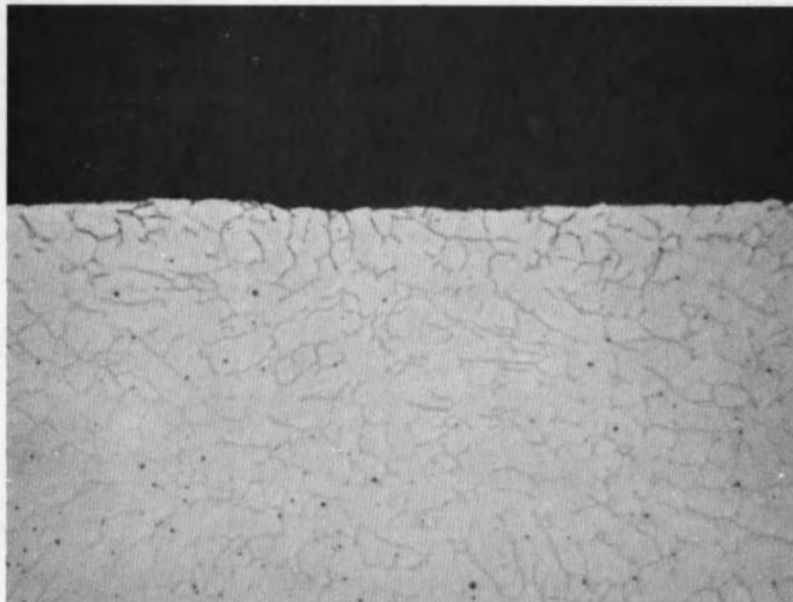


Fig. 15 Stainless Steel 304L, Stressed, at 308 Rod Weld, Exposed 720 hr to Cryodeposit, 2816 hr to Gas, 20 cycles, 500X



Fig. 16 Stainless Steel 304L, Stressed, at 347 Rod Weld, Exposed 720 hr to Cryodeposit, 2816hr to Gas, 20 cycles, 500X



Fig. 17 Stainless Steel 304L, at Resistance Spot Weld, Exposed 720 hr to Cryodeposit, 2816 hr to Gas, 20 cycles, 500X

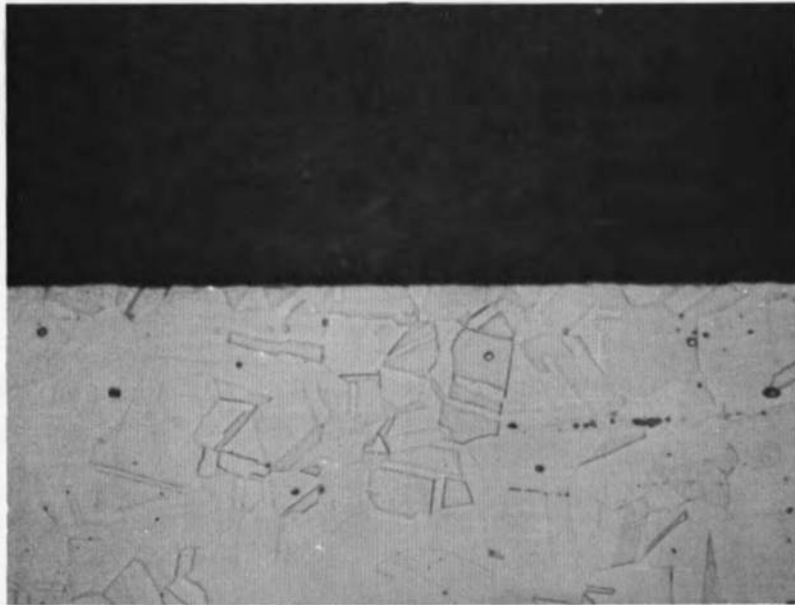


Fig. 18 Stainless Steel 304L, Welded with 304L Rod, Epoxy Coated, Exposed 58 hr to Cryodeposit, 441 hr to Gos, 9 cycles, 500X

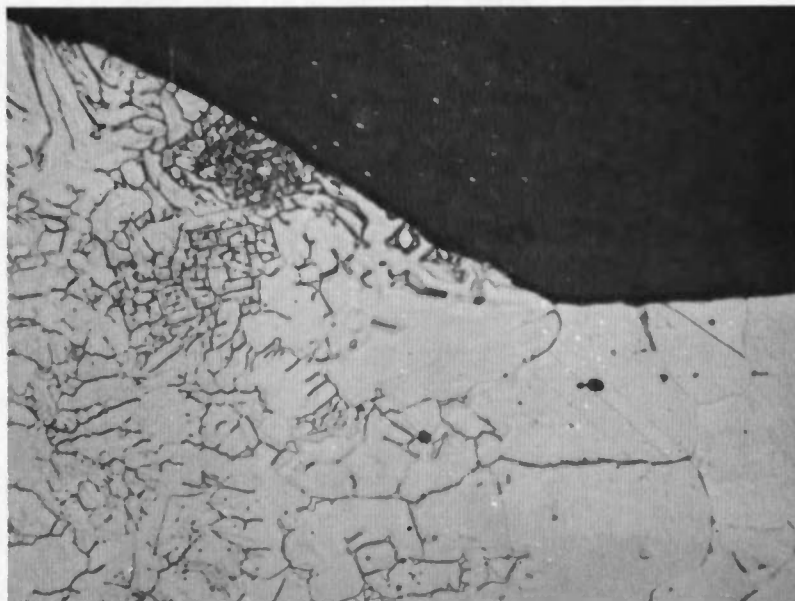


Fig. 19 Stainless Steel 304L, at 308 ELC Weld, Epoxy Coated, Exposed 58 hr to Cryodeposit, 441 hr to Gos, 9 cycles, 500X

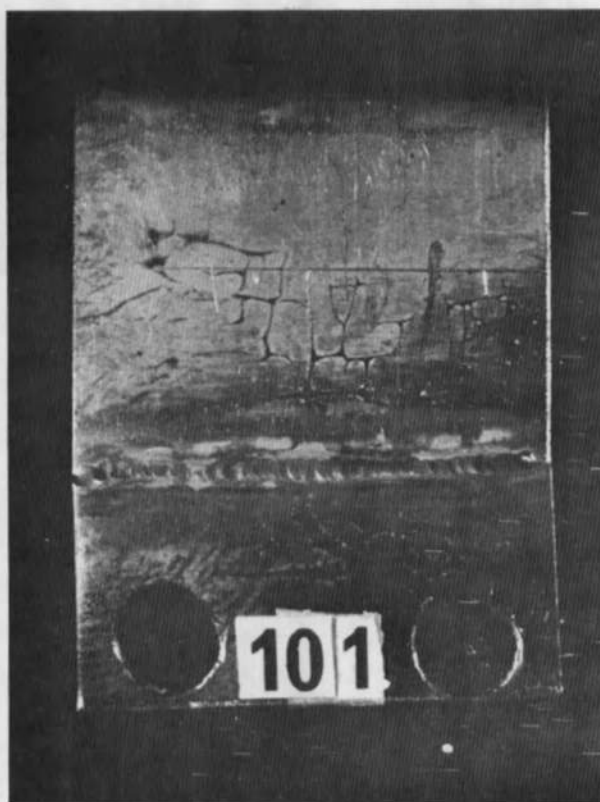


Fig. 20 Stainless Steel 304L, Fusion Welded, Exposed 420 hr to Cryodeposit, 1190 hr to Gas, 8 cycles, 3X

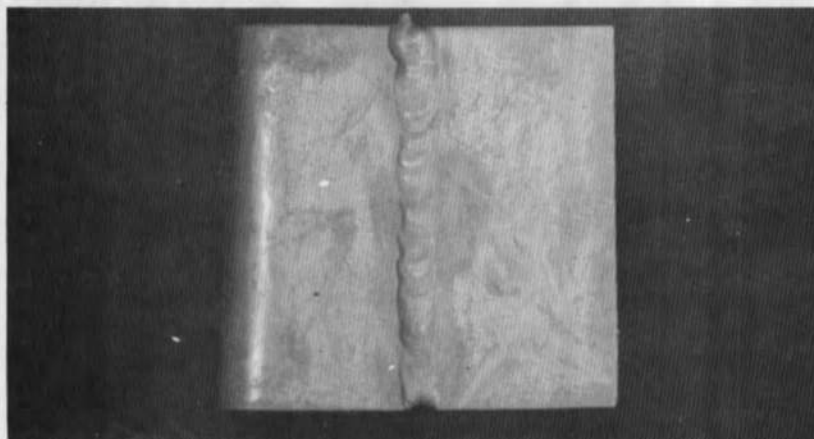


Fig. 21 Brazed Copper, Contacted Copper Fin, Exposed 58 hr to Cryodeposit, 441 hr to Gas, 9 cycles, 2X



Fig. 22 Control Specimen, Unbraided Copper, 500X



Fig. 23 Unbraided Copper, Contacted Copper Fin, Exposed 58 hr to Cryodeposit, 441 hr to Gas, 9 cycles, 500X



Fig. 24 Brozed Copper, Contacted Copper Fin, Exposed 420 hr to Cryodeposit, 1190 hr to Gas, 8 cycles, 500X



Fig. 25 Unbrozed Copper, Contacted Aluminum Fin, Exposed 720 hr to Cryodeposit, 2816 hr to Gas, 20 cycles, 500X

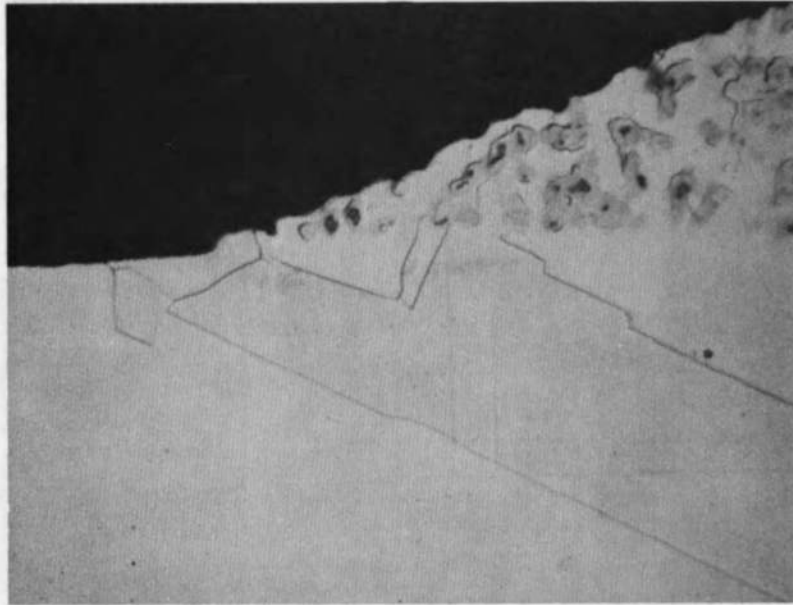


Fig. 26 Brazed Copper Control, at Broze Weld, 500X

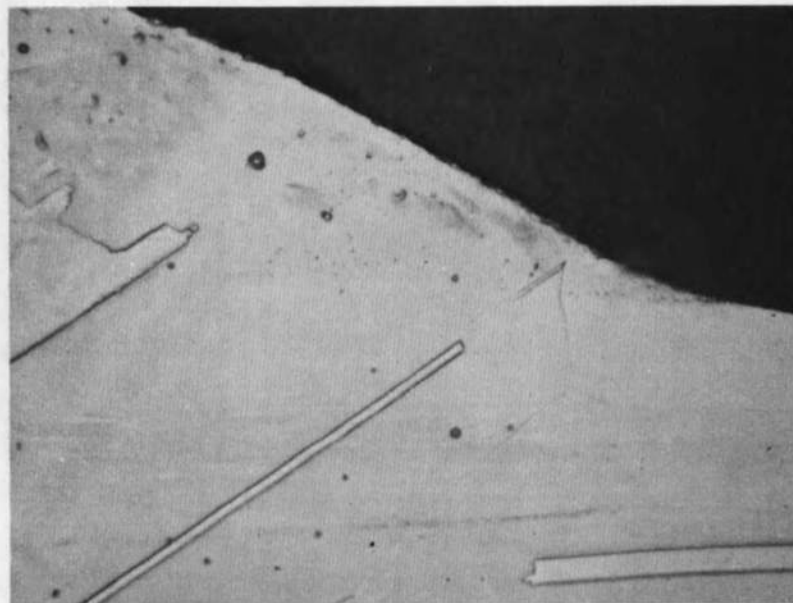


Fig. 27 Brazed Copper at Braze Weld, Exposed 58 hr to Cryodeposit, 441 hr to Gos, 9 cycles, 500X

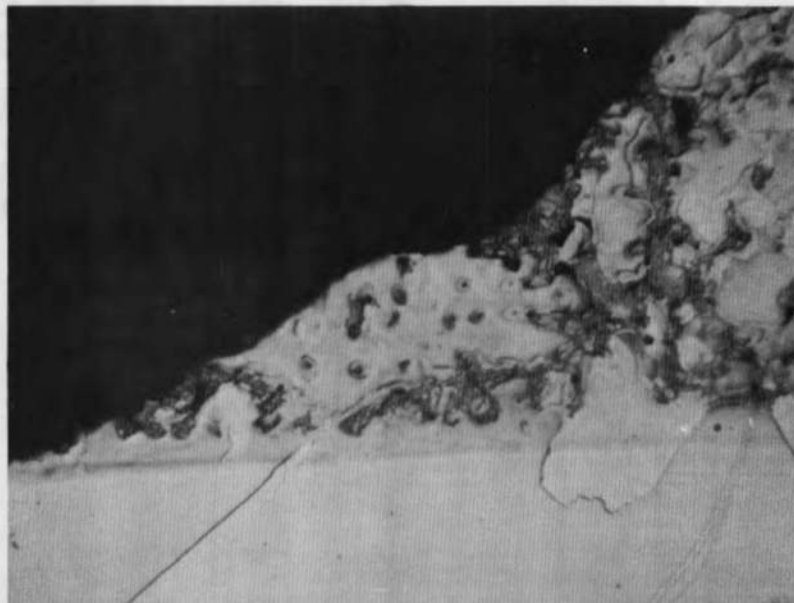


Fig. 28 Brazed Copper at Braze Weld, Exposed 420 hr to Cryodeposit, 1190 hr to Gas, 8 cycles, 500X

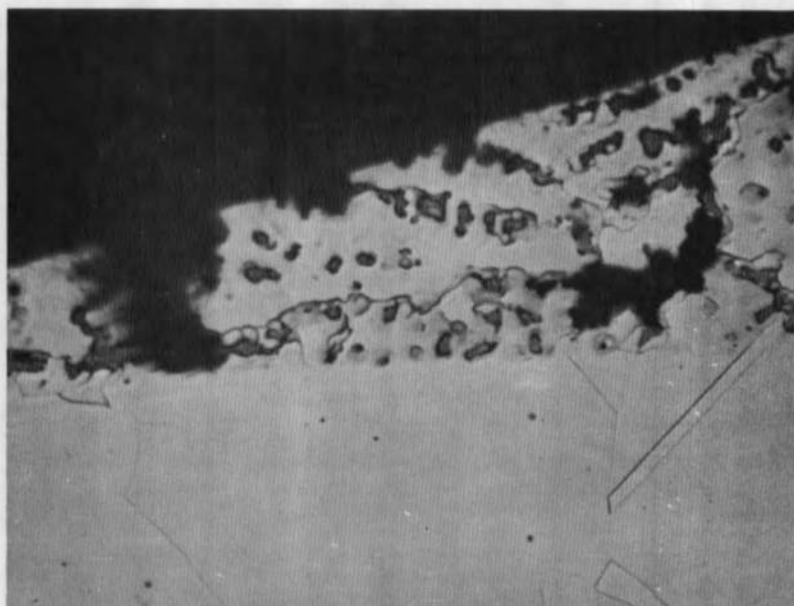


Fig. 29 Brazed Copper at Braze Weld, Exposed 720 hr to Cryodeposit, 2816 hr to Gas, 20 cycles, 500X

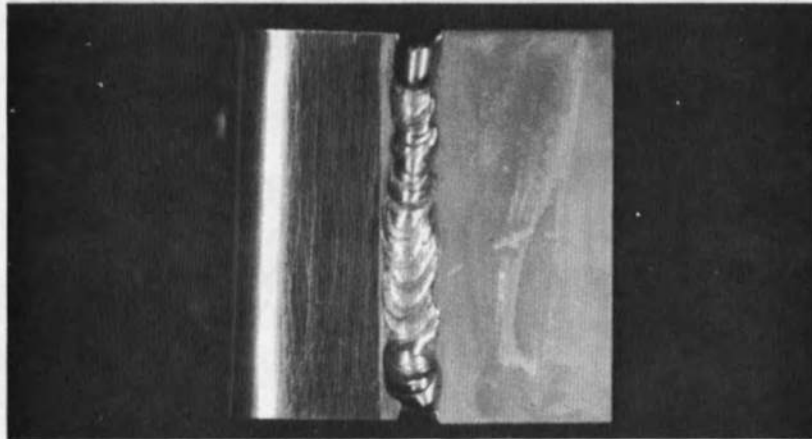


Fig. 30 Composite Specimen, Copper Tip, Exposed 58 hr to Cryodeposit, 441 hr to Gas, 9 cycles, 2X

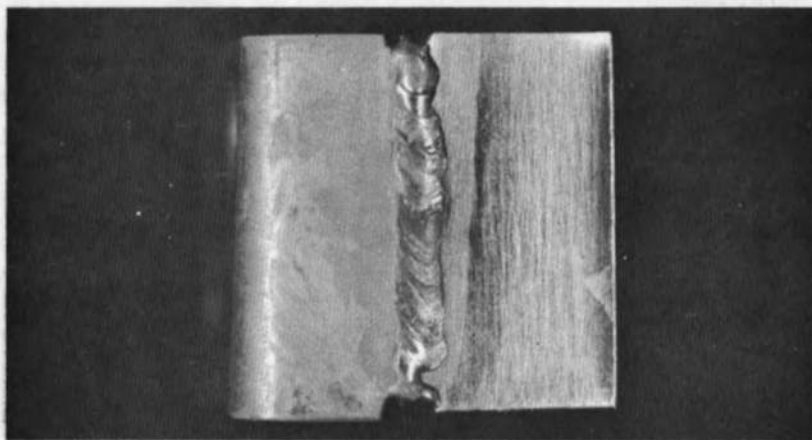


Fig. 31 Composite Specimen, Stainless Steel Tip, Exposed 58 hr to Cryodeposit, 441 hr to Gas, 9 cycles, 2X



Fig. 32 Composite Specimen, Stainless Steel Side, Exposed 58 hr to Cryodeposit, 441 hr to Gas, 9 cycles, Stressed, 500X

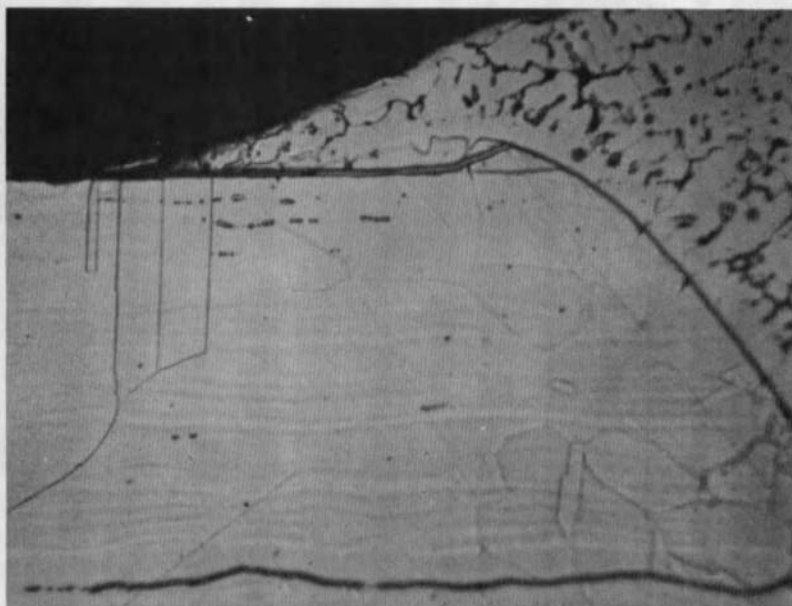


Fig. 33 Composite Specimen, at Weld on Stainless Steel Side, Exposed 58 hr to Cryodeposit, 441 hr to Gas, 9 cycles, Stressed, 500X

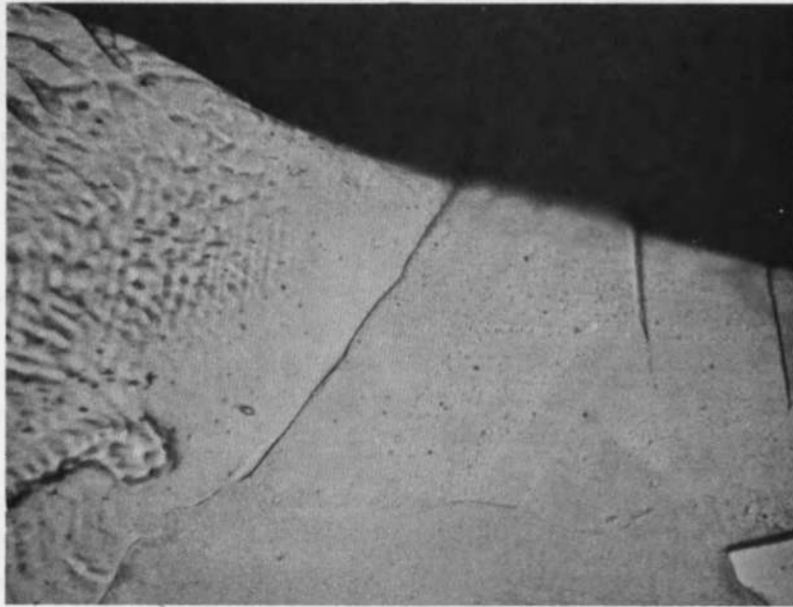


Fig. 34 Composite Specimen, at Weld on Copper Side, Exposed 58 hr to Cryodeposit, 441 hr to Gas, 9 cycles, Stressed, 500X



Fig. 35 Composite Specimen, Copper Side, Exposed 58 hr to Cryodeposit, 441 hr to Gas, 9 cycles, Stressed, 500X

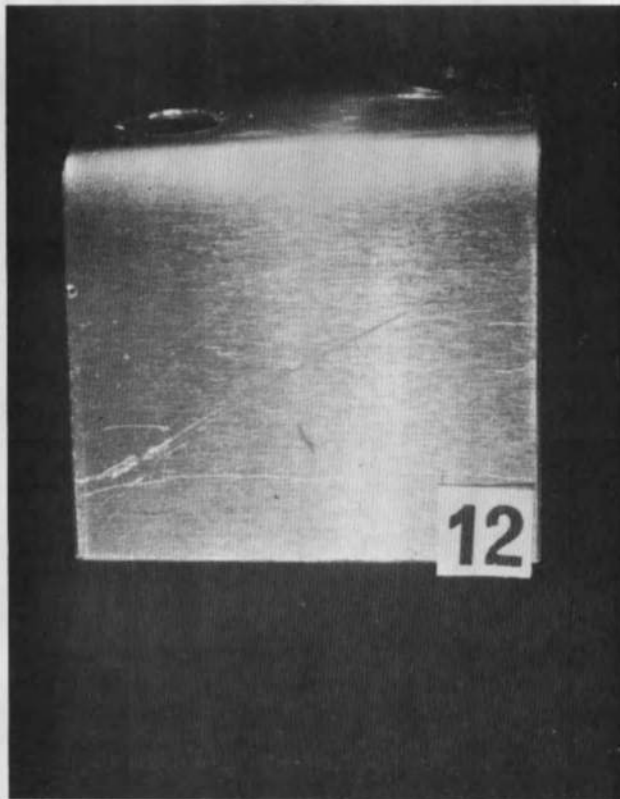


Fig. 36 Aluminum, Contacted Aluminum Fin, Exposed 720 hr to Cryodeposit, 2816 hr to Gas, 20 cycles, 3X

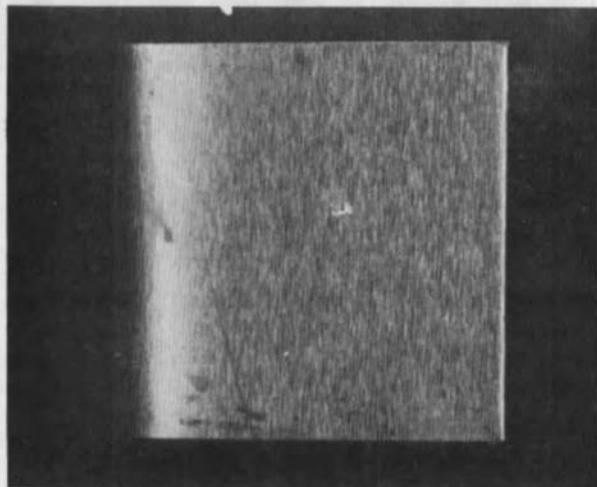


Fig. 37 Aluminum, Contacted Copper Fin, Exposed 58 hr to Cryodeposit, 441 hr to Gas, 9 cycles, 2X

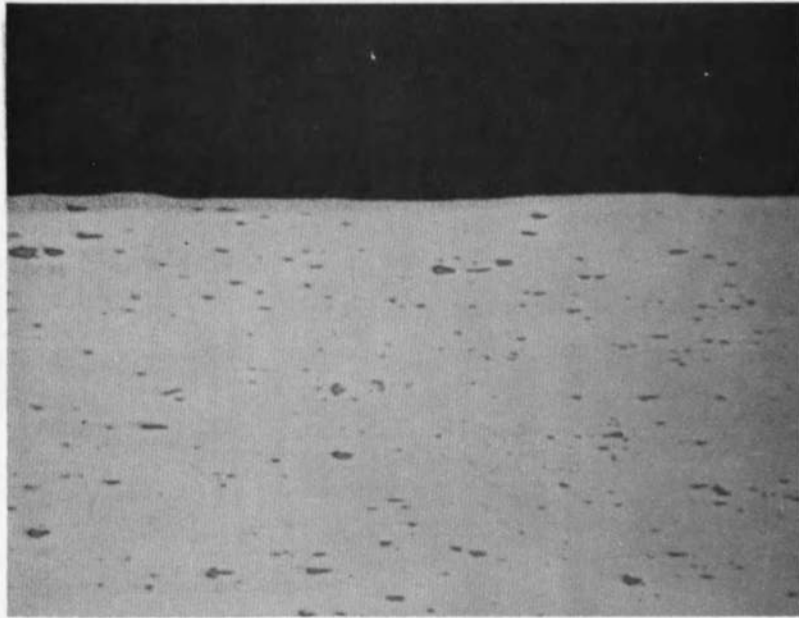
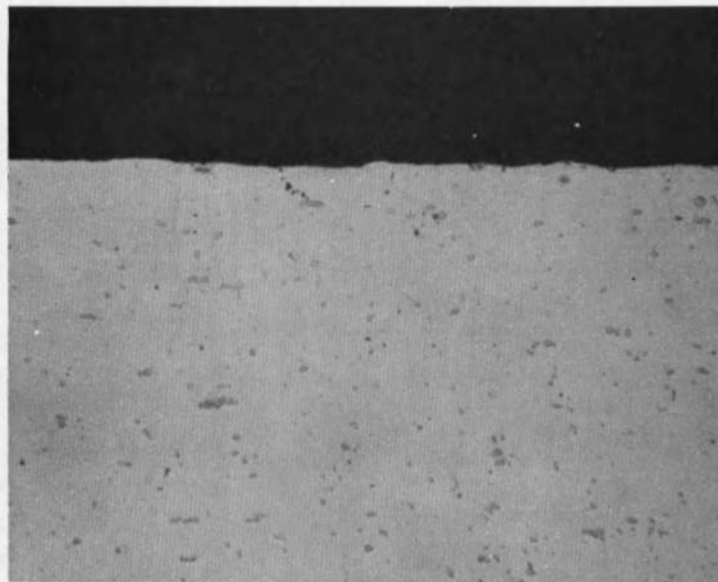


Fig. 38 Control Specimen, Aluminum, 500X



**Fig. 39 Aluminum, Contacted Copper Fin, Exposed 58 hr to Cryodeposit,
441 hr to Gas, 9 cycles, 500X**

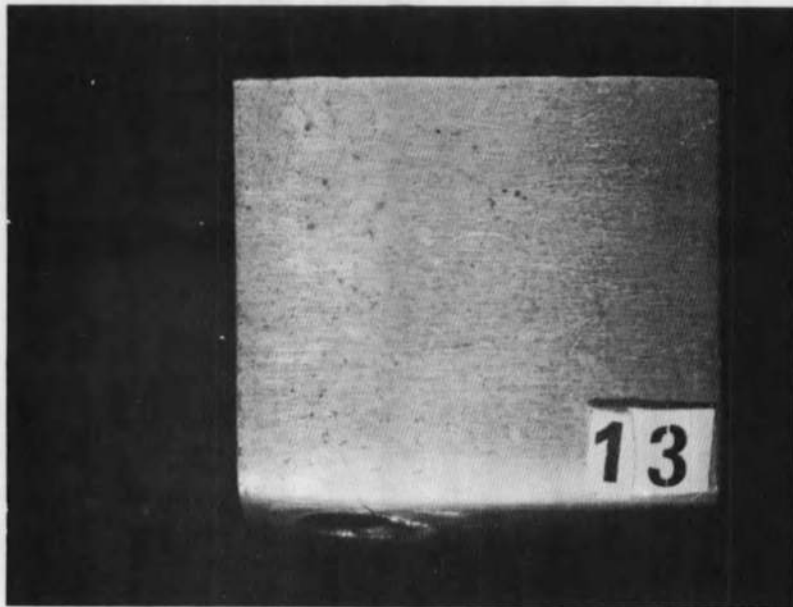


Fig. 40 Aluminum, Contacted Aluminum Fin, Exposed 720 hr to Cryodeposit, 2816 hr to Gas, 20 cycles, 3X

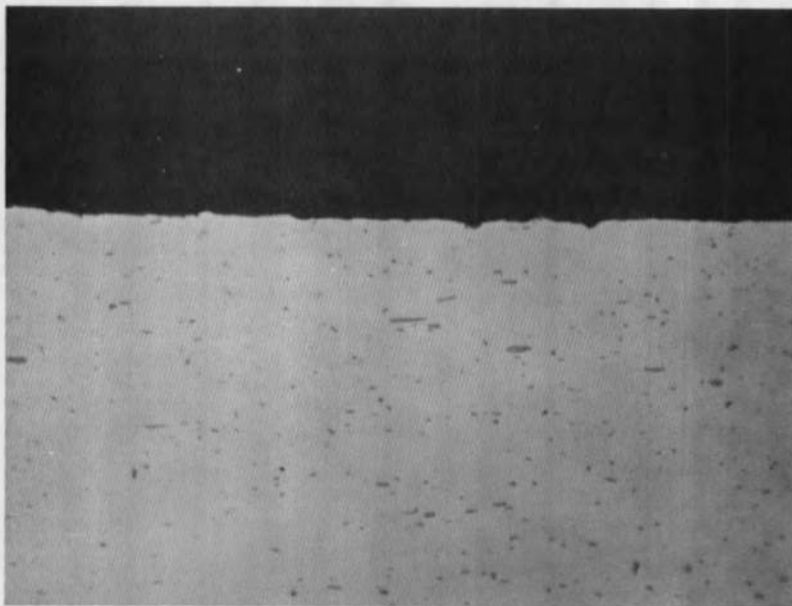


Fig. 41 Aluminum, Contacted Aluminum Fin, Exposed 720 hr to Cryodeposit, 2816 hr to Gas, 20 cycles, 500X

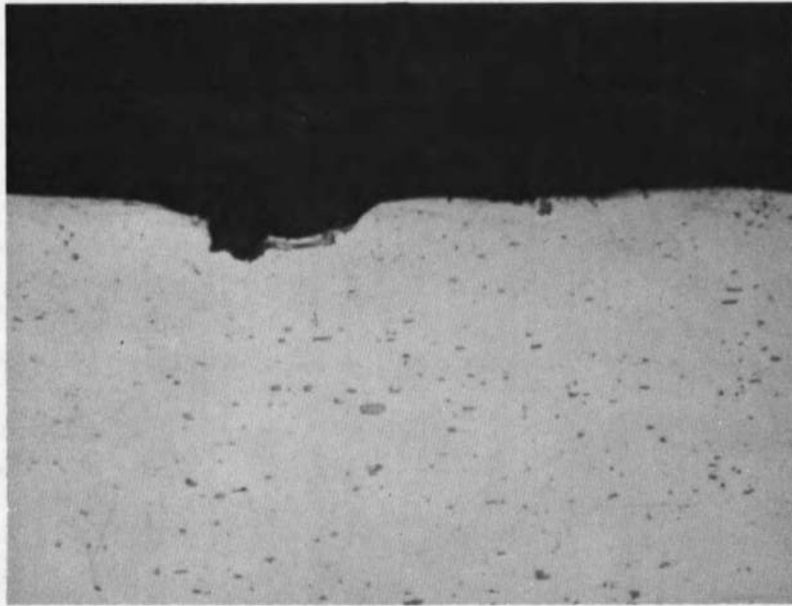


Fig. 42 Aluminum, Contacted Copper Fin, Exposed 720 hr to Cryodeposit, 2816 hr to Gas, 20 cycles, 500X

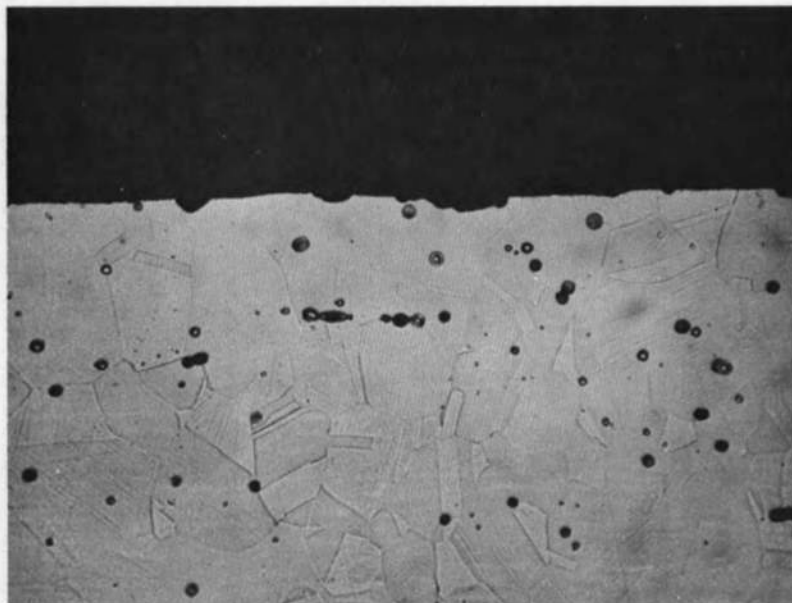


Fig. 43 Control Specimen, Stainless Steel Cryopanel Section, 500X

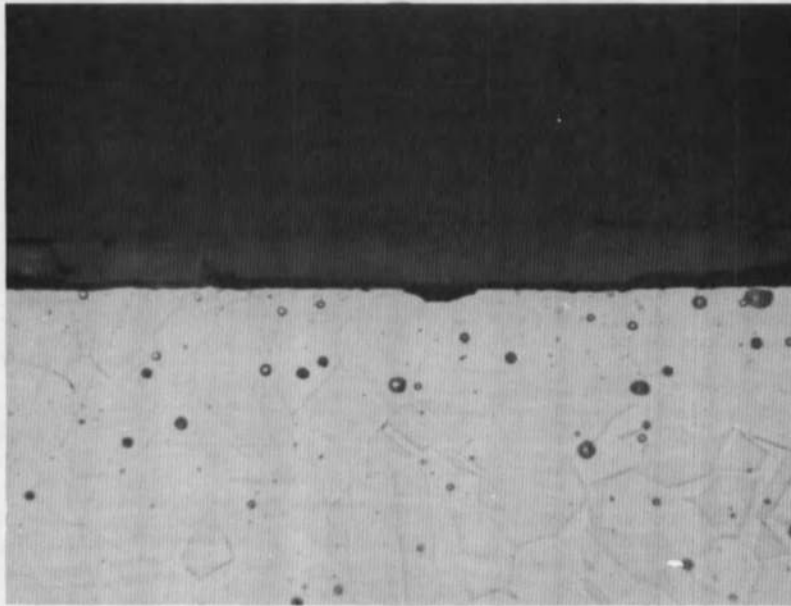


Fig. 44 Stainless Steel Cryopanel Specimen, Exposed 58 hr to Cryodeposit, 441 hr to Gas, 9 cycles, 500X

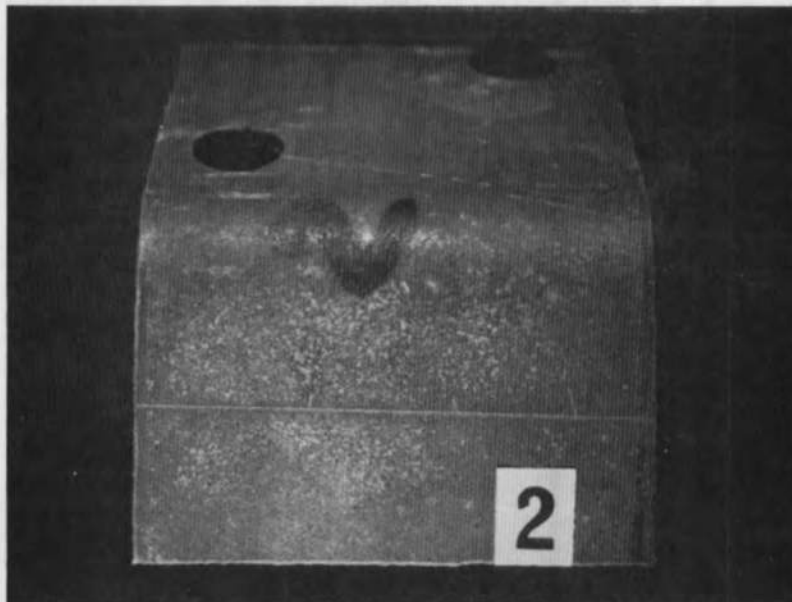


Fig. 45 Copper Cryopanel, Uncoated Side, Exposed 298 hr to Cryodeposit, 1629 hr to Gas, 12 cycles, 3X

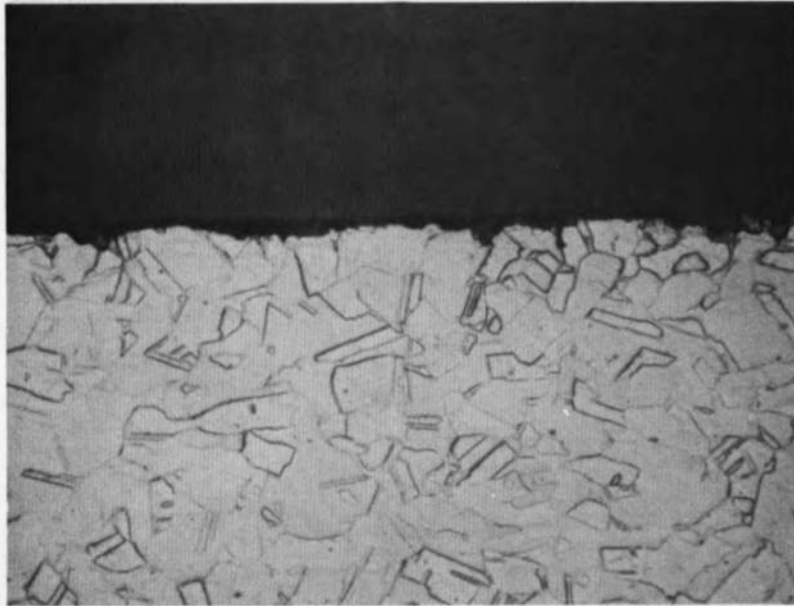


Fig. 46 Control Copper Cryopanel Specimen, Uncoated Side, 500X

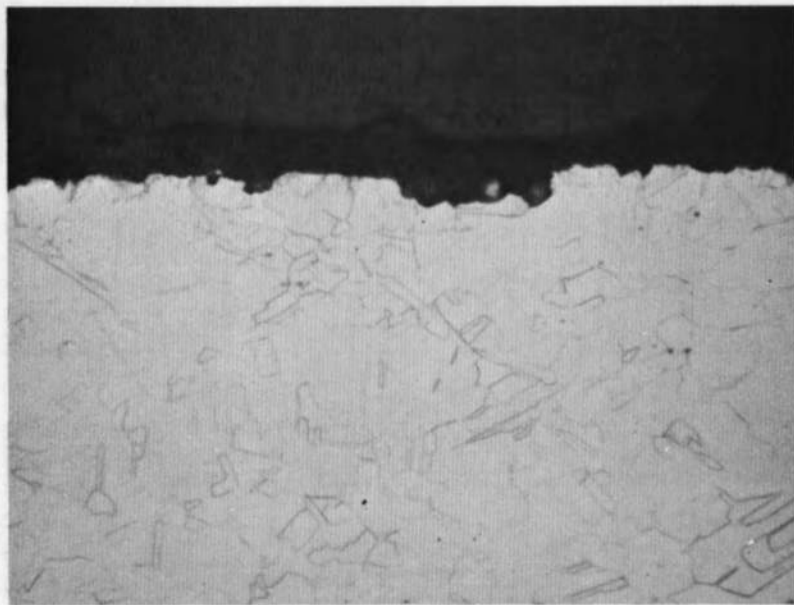


Fig. 47 Copper Cryopanel, Uncoated Side, Exposed 298 hr to Cryodeposit, 1629 hr to Gas, 12 cycles, 500X

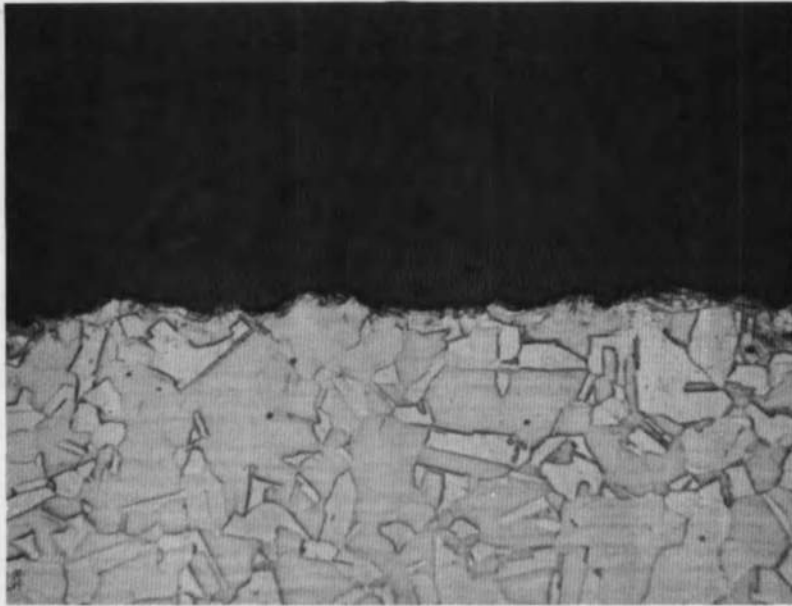
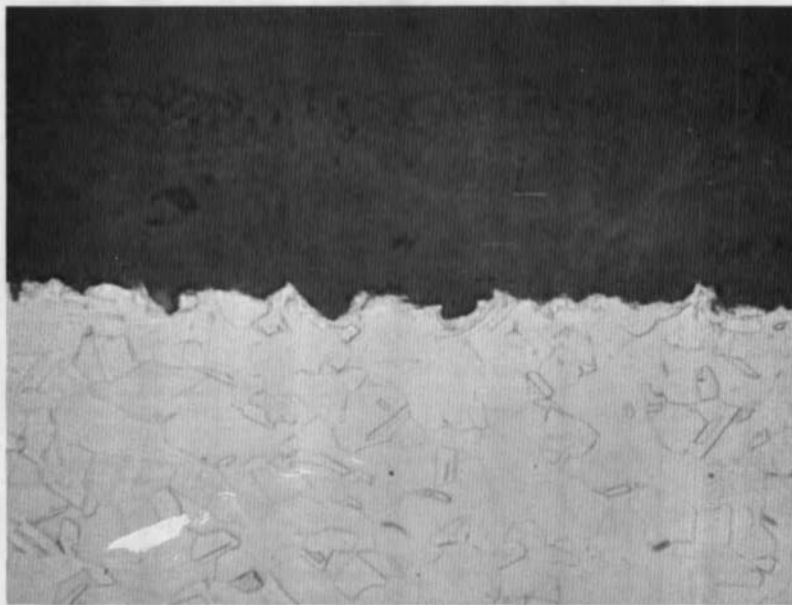


Fig. 48 Control Copper Cryopanel, Epoxy-Coated Side, 500X



**Fig. 49 Copper Cryopanel, Coated Side, Exposed 298 hr to Cryodeposit,
1629 hr to Gas, 12 cycles, 500X**

DOCUMENT CONTROL DATA - R & D

(Security classification of title, body of abstract and indexing annotation must be entered when the overall report is classified)

1. ORIGINATING ACTIVITY (Corporate author) Arnold Engineering Development Center, ARO, Inc., Operating Contractor, Arnold Air Force Station, Tennessee		2a. REPORT SECURITY CLASSIFICATION UNCLASSIFIED	
		2b. GROUP -----N/A	
3. REPORT TITLE NITROGEN TETROXIDE CORROSION STUDIES OF CRYOPANEL MATERIALS FOR SPACE CHAMBER PROPULSION TESTING			
4. DESCRIPTIVE NOTES (Type of report and Inclusive dates) May 1966 to May 1967 - Final Report			
5. AUTHOR(S) (First name, middle initial, last name) P. G. Waldrep and D. M. Trayer, ARO, Inc.			
6. REPORT DATE October 1968	7a. TOTAL NO. OF PAGES 58	7b. NO. OF REFS 12	
8a. CONTRACT OR GRANT NO. F40600-69-C-0001	9a. ORIGINATOR'S REPORT NUMBER(S) AEDC-TR-68-138		
b. PROJECT NO. 5730			
c. Program Element 6240518F	9b. OTHER REPORT NO(S) (Any other numbers that may be assigned this report) N/A		
d. Task 573004			
10. DISTRIBUTION STATEMENT This document has been approved for public release and sale; its distribution is unlimited.			
11. SUPPLEMENTARY NOTES Available in DDC.		12. SPONSORING MILITARY ACTIVITY AEDC (AETS), Air Force Systems Command, Arnold Air Force Station, Tennessee 37389	
13. ABSTRACT The corrosive action of nitrogen dioxide gas and nitrogen tetroxide cryodeposit on several cryopanel metals was investigated. The specimen temperatures were periodically cycled between 77 and 300°K. The nitrogen dioxide gas pressure at ambient temperature was 4 torr. Three tests were made at different exposure periods. The basic metals tested were aluminum 1100, phosphorus deoxidized copper, and type 304L stainless steel. Weldments were made in some copper and stainless steel specimens, and an external bending stress was placed on selected specimens during the test. The degree of corrosion detected was minor and would not likely result in any structural failure of cryopanel components under similar conditions. However, some loss of the optical properties of these materials may be expected.			

14

KEY WORDS

cryopanel metals

corrosion studies

²
nitrogen tetroxide -- Corrosion

³
space chambers -- Corrosion

temperature testing

15-2

1. Cryopanels -- Corrosion

LINK A

LINK B

LINK C

ROLE

WT

ROLE

WT

ROLE

WT